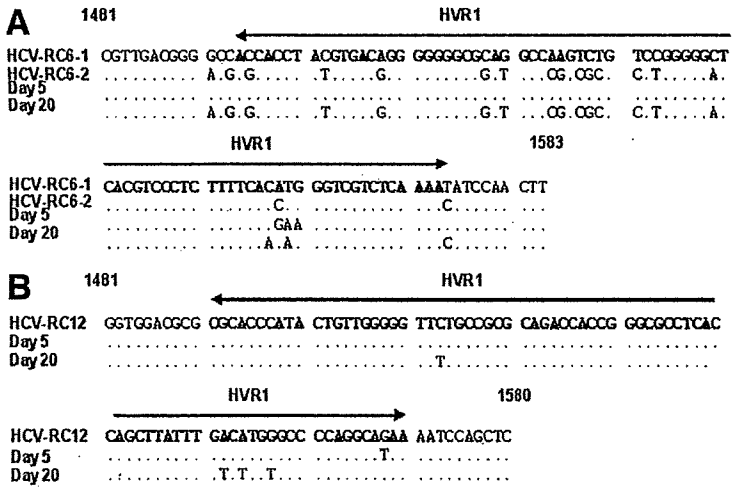

Fig. 4. Comparison of HCV-HVR1 sequences in the serum used for infection and the HCV replicating in the cells on days 5 and 20 after infection of HCV-RC6 (A) or HCV-RC12 (B). Nucleotide numbering was based on HCV-J1 sequence (GenBank Access. No. D10749). Three additional nucleotides were found at the 5′-terminal end of the E2 regions of all RC6 sequences. The major sequence present in the serum used for infection is shown in the upper row in each panel. Dots represent the identical nucleotides.

HCV-RC12-infected 3D-HuS-E/2 cells. LDH activity showed a strong correlation with HCV-RNA levels in the medium on day 10 p.i. in HCV-R12-infected cells (Fig. 3B), suggesting a cytotoxic effect of HCV-RC12 that was not observed in the case of HCV-RC6 (Fig. 3A,C). To determine if this HCV infection-mediated cytotoxicity is due to apoptosis, as with other viruses belonging to the Flaviviridae family,[19] the involvement of caspase was examined using the caspase inhibitor z-VAD-fmk. A significant dose-dependent reduction in HCV-RNA levels in the medium and LDH activity (Fig. 5A,B) was found, whereas no significant effect was observed on the viability of noninfected cells (Fig. 5B) or intracellular HCV-RNA levels (Fig. 5A). This suggested that the cytotoxic effect of HCV infection is mediated by apoptosis. It is noteworthy that HCV-induced cytopathicity was also found when HCV-P17 and HCV-P33 samples were used for infection (both are HCV-2a genotype) and was not reproduced in any of the HCV-1b genotype samples used in this work (Fig. 5C).

After infection with HCV-RC6, no cytotoxicity was detected that might have inhibited HCV-RC6-1 proliferation in the cells. However, HCV-RC6-2 RNA replaced HCV-RC6-1 RNA during prolonged culture. To assess a

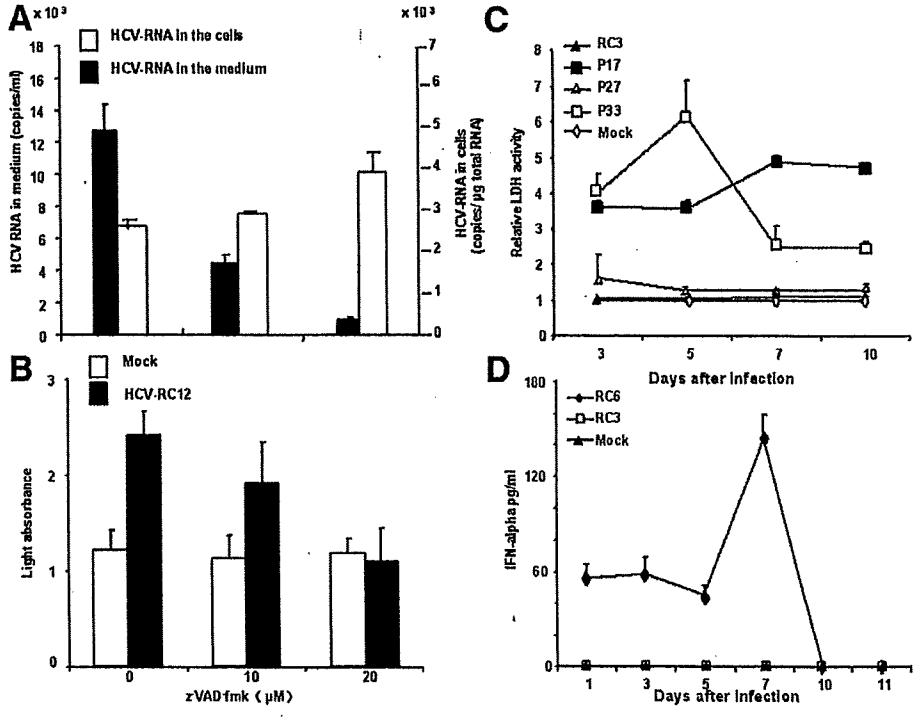

Fig. 5. Cellular response of 3D-HuS-E/2 cells infected with bbHCV. 3D-HuS-E/2 cells infected with HCV-RC12 and mock-treated cells were cultured for 10 days in the presence of z-VAD-fmk (0, 10, and 20 μM). (A) HCV-RNA in the cells and medium on day 10 was measured as in Fig. 1. (B) LDH levels in the medium on day 10 after infection with HCV-RC12 was measured as in Fig. 3. (C) Culture media of HCV-RC3, HCV-P17, HCV-P27, HCV-P33, and mock-infected cells collected at designated points were used for the detection of LDH levels. (D) IFN-α levels in the culture media of HCV-RC6, HCV-RC3, and mock-infected cells collected at each designated timepoint were measured by ELISA. Data represent the mean ± SD of three independent experiments.

possible role of the innate-immune response in this phenomenon, the production of IFN-α in the medium was measured during the first 11 days p.i. IFN-α production was detected as early as day 1 p.i., reached a peak at day 7 p.i., and was then rapidly lost (Fig. 5D). These data suggest that HCV-RC6-1 infection induced the innate-immune response of the cells, possibly leading to suppression of its proliferation. In contrast to HCV-RC6-1, HCV-RC3 did not show any stimulation of IFN-α production upon infection in the first 10 days, showing a possible strain-dependent evasion from the host defense within the same genotype.

Discussion

In this study we report the development of a novel system that reproduces bbHCV infection, proliferation, and production of infectious virus. The most recent models used in the study of the life cycle of HCV infection are based on subclones of HuH-7 cells infected with JFH1 recombinant virus or its derivatives.[4] HuH-7 cells and its subclones, however, do not support the entire life cycle of the bbHCVs present in patients' blood.[5] Moreover, HCV has considerable diversity and variability. It is generally classified into six major genotypes and more than 100 subtypes.[20] This huge pool of natural HCV variants causes a wide variety of diseases, including chronic hepatitis, cirrhosis, and hepatocellular carcinoma.[21] JFH1, however, is a single isolate of HCV genotype 2a that was originally derived from a patient with rare fulminant hepatitis.[4] We suggest that our newly established system has an important advantage because it supports the entire life cycle of a variety of HCV strains and genotypes.

Due to the lack of some *in vivo* factors, including host immune response, *in vitro* systems may not completely reproduce the *in vivo* situation. However, *in vitro* experimental systems seem to be important to simplify particular events from the complex situation *in vivo*. From that standpoint, our cell culture system is likely reproducing the early event of HCV infection in the absence of host-immune responses and supporting whole life cycle of the blood-borne HCV. Several *in vitro* hepatocyte culture systems have been reported to be useful for studying the infection and replication of bbHCV.[5-8,22] Only the radial-flow bioreactor (RFB) 3D culture system demonstrated production of infectious viruses.[22] In our studies we observed not only the enhancement of HCV replication, but also the production of infectious HCV particles in the medium using the 3D/HF system. These data suggest that some structure of the cell mass formed by the 3D culture system, most likely the polar character, is essential for the life cycle of bbHCV. The RFB system is composed of a dedicated device containing 1×10^9 FLC4 cells with a culture area of 2.7 m^2.[22] It can only be used to study HCV particle production in the medium and not the cellular events that accompany the HCV life cycle. In contrast, because cells grown in our 3D/HF system are cultured in 12-well plates at a density of 3×10^5/fiber, it is much simpler to study both viral and cellular events.

The production of infectious particles was not detected with infection by different HCV strains, despite detecting equivalent levels of HCV-RNA in the cells (Fig. 1B,C). Delayed production of infectious particles was also observed in cells infected with HCV-RC12 after prolonged culture. A similar delay was also observed in the RFB system.[22] Considering the relative stability of HuS-E/2 cells[5] and the relatively high frequency of the change in HCV population in the cells,[16] it is likely that mutation of the HCV genome and/or selection of clones during prolonged culture improved the productivity of infectious particles. A marked improvement of infectious particle production by substitution of the structural proteins of the genome was also reported in the recombinant HCV production system.[23] The lack of production of infectious particles soon after infection may serve to avoid an early strong response from the host immune system, and demonstrates a novel mechanism of latent infection by HCV. Although they may not be associated with plasma components as those present *in vivo*, HCV virus-like particles produced by this system showed a close resemblance to those isolated from infected HCV patients because they showed the same size[18] and were within the fraction range.[24] They may help in the study of viral and cellular factors required for particle production and the possible receptors utilized for infection with different HCV strains.

Fluctuation in HCV proliferation was observed during the prolonged culture of 3D-HuS-E/2 cells infected with bbHCV (Fig. 3A,B), consistent with previous reports in other culture systems.[6,22] This fluctuation was associated with a change in viral quasispecies, suggesting that an HCV strain having a growth advantage proliferates selectively and dominantly in these culture conditions. Because the progressive emergence of each dominant strain was only temporary, it is highly likely that the infection and proliferation of such an HCV strain is suppressed by cellular mechanism(s). Our results suggest that there are actually two cellular mechanisms functioning to do this. The first is the involvement of the innate immune system, as evidenced by the secretion of IFN-α during the first week of infection (Fig. 5D). This is the first report of secretion of IFN-α from cultured cells infected with bbHCV. Although recent reports suggest that stimulation of the IFN pathway by HCV infection could be impaired by HCV NS3-4a proteinase-mediated cleavage of IPS-

1,[25] our results suggest that not all bbHCVs possess a host cell suppressive function. The second mechanism is HCV-induced cell death (Fig. 3C). Almost all the studies reporting HCV-induced apoptosis used hepatocellular carcinoma cell lines.[26,27] Because it has been established that the inability to undergo apoptosis is essential for the development of cancer,[28-30] our use of immortalized, noncancerous HuS-E/2 hepatocytes may make it possible to reproduce the physiological response of the cells to bbHCV infection more closely. Although HCV-induced apoptosis was not found when HCV-1b was used for infection, it was found in all cases where HCV-2a was used, suggesting a higher cytopathic tendency of the HCV-2a genotype. HCV proliferation was continuously found even after the suppression of the first peak of RNA production during prolonged culture. How HCV survives under those conditions is still unknown. Further studies to clarify the molecular mechanisms involving the HCV-cell interaction can be done using this novel 3D culture system that reproduces the infection of a variety of bbHCVs.

In conclusion, we have established a new *in vitro* culture system that can support the entire life cycle of a variety of HCV isolates and genotypes. Although this *in vitro* model system may not completely reproduce the *in vivo* situation, we believe it is the first *in vitro* system showing HCV strain-dependent virus/cell interaction including induction of cellular apoptosis and/or evasion from cellular innate immune response, which may make it a good tool for analysis of virus/host interaction together with the development of new anti-HCV strategies for the different bbHCV strains.

Acknowledgment: We thank T. Yamaguchi for providing hollow fibers and culture medium.

References

1. Wasley A, Alter MJ. Epidemiology of hepatitis C: geographic differences and temporal trends. Semin Liver Dis 2000;20:1-16.
2. Younossi Z, Kallman J, Kincaid J. The effects of HCV infection and management on health-related quality of life. HEPATOLOGY 2007;45:806-816.
3. Fried MW, Shiffman ML, Reddy KR, Smith C, Marinos G, Goncales FL Jr, et al. Peginterferon alfa-2a plus ribavirin for chronic hepatitis C virus infection. N Engl J Med 2002;347:975-982.
4. Wakita T, Pietschmann T, Kato T, Date T, Miyamoto M, Zhao Z, et al. Production of infectious hepatitis C virus in tissue culture from a cloned viral genome. Nat Med 2005;11:791-796.
5. Aly HH, Watashi K, Hijikata M, Kaneko H, Takada Y, Egawa H, et al. Serum-derived hepatitis C virus infectivity in interferon regulatory factor-7-suppressed human primary hepatocytes. J Hepatol 2007;46:26-36.
6. Ikeda M, Sugiyama K, Mizutani T, Tanaka T, Tanaka K, Sekihara H, et al. Human hepatocyte clonal cell lines that support persistent replication of hepatitis C virus. Virus Res 1998;56:157-167.
7. Chong TW, Smith RL, Hughes MG, Camden J, Rudy CK, Evans HL, et al. Primary human hepatocytes in spheroid formation to study hepatitis C infection. J Surg Res 2006;130:52-57.
8. Molina S, Castet V, Pichard-Garcia L, Wychowski C, Meurs E, Pascussi JM, et al. Serum-derived hepatitis C virus infection of primary human hepatocytes is tetraspanin CD81 dependent. J Virol 2008;82:569-574.
9. El-Farrash MA, Aly HH, Watashi K, Hijikata M, Egawa H, Shimotohno K. In vitro infection of immortalized primary hepatocytes by HCV genotype 4a and inhibition of virus replication by cyclosporin. Microbiol Immunol 2007;51:127-133.
10. Mizumoto H, Ishihara K, Nakazawa K, Ijima H, Funatsu K, Kajiwara T. A new culture technique for hepatocyte organoid formation and long-term maintenance of liver-specific functions. Tissue Eng Part C Methods 2008; 14:167-175.
11. Funatsu K, Ijima H, Nakazawa K, Yamashita Y, Shimada M, Sugimachi K. Hybrid artificial liver using hepatocyte organoid culture. Artif Organs 2001;25:194-200.
12. Mizumoto H, Aoki K, Nakazawa K, Ijima H, Funatsu K, Kajiwara T. Hepatic differentiation of embryonic stem cells in HF/organoid culture. Transplant Proc 2008;40:611-613.
13. Andrei G. Three-dimensional culture models for human viral diseases and antiviral drug development. Antiviral Res 2006;71:96-107.
14. Hijikata M, Kato N, Ootsuyama Y, Nakagawa M, Ohkoshi S, Shimotohno K. Hypervariable regions in the putative glycoprotein of hepatitis C virus. Biochem Biophys Res Commun 1991;175:220-228.
15. Boulestin A, Sandres-Saune K, Payen JL, Altic L, Dubois M, Pasquier C, et al. Genetic heterogeneity of the envelope 2 gene and eradication of hepatitis C virus after a second course of interferon-alpha. J Med Virol 2002; 68:221-228.
16. Murakami K, Inoue Y, Hmwe SS, Omata K, Hongo T, Ishii K, et al. Dynamic behavior of hepatitis C virus quasispecies in a long-term culture of the three-dimensional radial-flow bioreactor system. J Virol Methods 2008;148:174-181.
17. Meuleman P, Hesselgesser J, Paulson M, Vanwolleghem T, Desombere I, Reiser H, et al. Anti-CD81 antibodies can prevent a hepatitis C virus infection in vivo. HEPATOLOGY 2008;48:1761-1768.
18. Kaito M, Watanabe S, Tsukiyama-Kohara K, Yamaguchi K, Kobayashi Y, Konishi M, et al. Hepatitis C virus particle detected by immunoelectron microscopic study. J Gen Virol 1994;75:1755-1760.
19. Roulston A, Marcellus RC, Branton PE. Viruses and apoptosis. Annu Rev Microbiol 1999;53:577-628.
20. Forns X, Bukh J. The molecular biology of hepatitis C virus. Genotypes and quasispecies. Clin Liver Dis 1999;3:693-716, vii.
21. Dickson RC. Clinical manifestations of hepatitis C. Clin Liver Dis 1997; 1:569-585.
22. Aizaki H, Nagamori S, Matsuda M, Kawakami H, Hashimoto O, Ishiko H, et al. Production and release of infectious hepatitis C virus from human liver cell cultures in the three-dimensional radial-flow bioreactor. Virology 2003;314:16-25.
23. Mateu G, Donis RO, Wakita T, Bukh J, Grakoui A. Intragenotypic JFH1 based recombinant hepatitis C virus produces high levels of infectious particles but causes increased cell death. Virology 2008;376:397-407.
24. Li X, Jeffers LJ, Shao L, Reddy KR, de Medina M, Scheffel J, et al. Identification of hepatitis C virus by immunoelectron microscopy. J Viral Hepat 1995;2:227-234.
25. Gale M Jr, Foy EM. Evasion of intracellular host defence by hepatitis C virus. Nature 2005;436:939-945.
26. Fischer R, Baumert T, Blum HE. Hepatitis C virus infection and apoptosis. World J Gastroenterol 2007;13:4865-4872.
27. Aoki H, Hayashi J, Moriyama M, Arakawa Y, Hino O. Hepatitis C virus core protein interacts with 14-3-3 protein and activates the kinase Raf-1. J Virol 2000;74:1736-1741.
28. Ladu S, Calvisi DF, Conner EA, Farina M, Factor VM, Thorgeirsson SS. E2F1 inhibits c-Myc-driven apoptosis via PIK3CA/Akt/mTOR and COX-2 in a mouse model of human liver cancer. Gastroenterology 2008; 135:1322-1332.
29. Lowe SW, Lin AW. Apoptosis in cancer. Carcinogenesis 2000;21:485-495.
30. Schulze-Bergkamen H, Krammer PH. Apoptosis in cancer—implications for therapy. Semin Oncol 2004;31:90-119.

Biochemical and Biophysical Research Communications 379 (2009) 330–334

Contents lists available at ScienceDirect

Biochemical and Biophysical Research Communications

journal homepage: www.elsevier.com/locate/ybbrc

3D cultured immortalized human hepatocytes useful to develop drugs for blood-borne HCV

Hussein Hassan Aly [a], Kunitada Shimotohno [b], Makoto Hijikata [a,c,*]

[a] Laboratory of Human Tumor Viruses, The Institute for Virus Research, Kyoto University, Department of Viral Oncology, 53 Kawaharacho, Shogoin, Sakyoku, Kyoto 606-8507, Japan
[b] Center for Human Metabolomic Systems Biology, Keio University, 35 Shinano-machi, Shinjuku-ku, Tokyo 160-8582, Japan
[c] Laboratory of Viral Oncology, Graduate School of Biostudies, Kyoto University, Konoecho, Yoshida, Sakyoku, Kyoto 606-8501, Japan

ARTICLE INFO

Article history:
Received 5 December 2008
Available online 25 December 2008

Keywords:
Hepatitis C virus
Infection
Replication
3D culture
PPAR
Immortalized hepatocytes
Blood-borne HCV

ABSTRACT

Due to the high polymorphism of natural hepatitis C virus (HCV) variants, existing recombinant HCV replication models have failed to be effective in developing effective anti-HCV agents. In the current study, we describe an *in vitro* system that supports the infection and replication of natural HCV from patient blood using an immortalized primary human hepatocyte cell line cultured in a three-dimensional (3D) culture system. Comparison of the gene expression profile of cells cultured in the 3D system to those cultured in the existing 2D system demonstrated an up-regulation of several genes activated by peroxisome proliferator-activated receptor alpha (PPARα) signaling. Furthermore, using PPARα agonists and antagonists, we also analyzed the effect of PPARα signaling on the modulation of HCV replication using this system. The 3D *in vitro* system described in this study provides significant insight into the search for novel anti-HCV strategies that are specific to various strains of HCV.

© 2008 Elsevier Inc. All rights reserved.

Infection with Hepatitis C virus (HCV) is a serious health problem worldwide and leads to high rates of liver cirrhosis and hepatocellular carcinoma [1]. Given that the standard HCV therapy remains insufficient for the successful treatment of many patients [2], the development of more effective and less toxic anti-HCV agents is required. *In vitro* systems like the HCV replicon-bearing cells and the infectious particle-producing JFH1 system, has contributed to the discovery of new targets for anti-HCV therapy. However, these recombinant HCV genomes only proliferate in sublines of HuH-7 cells, which do not permit infection or proliferation of blood-borne HCV. Due to the high polymorphism of natural HCV, data from recombinant HCV systems could be evaluated by studying the therapeutic response of a variety of naturally occurring HCVs. However, the current systems available for such study remain insufficient due to the low infection and replication efficiency of the natural HCV strains.

More recently, production and secretion of infectious HCV particles has been reported in two independent three-dimensional (3D) cell culture systems, termed the radial-flow bioreactor (3D/RFB) and the thermoreversible gelatin polymer (3D/TGP) systems. These results were not observed in monolayer cultures [3], suggesting that hepatocytes cultured in 3D more closely resemble liver cells *in vivo* [4] and thus support HCV proliferation. In addition, analysis of gene expression levels in 3D cultured cells revealed that the newly established immortalized human hepatocyte (HuS-E/2 cells) gene profile was altered to more closely resemble that of human liver tissue when the cells were cultured in 3D/TGP [5].

In the current study, we cultured HuS-E/2 cells in 3D/TGP and demonstrated efficient proliferation of natural HCV. Furthermore, gene expression analysis of these cells demonstrated the activation of the peroxisome proliferators-activated receptor α (PPARα) signaling pathway, suggesting an important role for this pathway in the replication of natural HCV. Thus, the *in vitro* system described appears to be a useful tool for the study of HCV infection and proliferation as well as for the development of effective anti-viral agents against various natural HCVs.

Materials and methods

Cell culture. Immortalized human hepatocytes (HuS-E/2) and LucNeo#2 replicon cells [6] were cultured as previously described [5,7]. For the 3D-TGP culture system, 1×10^5 HuS-E/2 cells were cultured in 1 ml Mebiol gel (Mebiol Inc., Kanagawa, Japan)/well in 12-well plates. Five hundred microliters of fresh medium was overlaid on the solidified gel, and was changed every 2 days. Cell

* Corresponding author. Address: Laboratory of Human Tumor Viruses, The Institute for Virus, Kyoto University, Department of Viral Oncology, 53 Kawaharacho, Shogoin, Sakyoku, Kyoto 606-8507, Japan. Fax: +81 75 751 3998.
E-mail address: mhijikat@virus.kyoto-u.ac.jp (M. Hijikata).

0006-291X/$ - see front matter © 2008 Elsevier Inc. All rights reserved.
doi:10.1016/j.bbrc.2008.12.054

extraction from the gel was done at the designated time points according to the manufacturer's protocol.

RNA extraction, reverse transcriptase polymerase chain reaction (RT-PCR) and real-time RT-PCR (Q-PCR). At the designated time points, total cellular RNA was extracted and 1 μg of total RNA was used as a template for RT-PCR and for the quantitative detection of HCV-RNA using real-time RT-PCR (Q-PCR) as previously described [10].

HCV infection experiment. HCV infection experiments were carried out using sera from patients infected with HCV. Infection in 2D culture was undertaken as previously described [5]. For 3D/TGP cultured cells, the gel was solidified, and 50 μl HCV-containing patient serum with a titer of 1×10^6 HCV-RNA/ml was added to the culture and mixed. The culture was continued until the cells were extracted. Following extraction from 3D-TGP, cells were centrifuged and washed three times thoroughly with PBS. RNA was then extracted from the cells as described above. HCV infection into HuS-E/2 cells was also examined in the presence of anti-E2 mouse monoclonal antibody (917) as outlined previously [8].

Treatment of cells with PPARα signaling agonists and antagonists. Fenofibrate or MK886 (Sigma–Aldrich, USA) were added to the culture medium of HuS-E/2 (2D-HuS-E/2) cells from day 0 of HCV infection; or the culture medium of LucNeo#2 replicon harboring cells. The cells were then cultured to the designated time point.

Microarray analysis. Gene expression profiles of 3D/TGP cultured HuS-E/2 cells were obtained by microarray analysis (3D-Genes Human 25, Toray, Tokyo, Japan) and compared to those of cells cultured in 2D.

Results

3D/TGP cultures enhance HCV proliferation in HuS-E/2 cells

Infection and proliferation of the HCV genotype 1b (HCV-RC5) derived from the serum of patient RC5 in HuS-E/2 cells cultured in 3D/TGP (3D/TGP-HuS-E/2 cells) was investigated and compared with that of HuS-E/2 cells cultured in 2D (2D-Hus-E/2). As outlined in Fig. 1A, the HCV-RNA levels in the 3D/TGP-HuS-E/2 cells were significantly higher at all of the time points examined following infection than in the 2D-HuS/E2 cells, suggesting that the 3D/TGP system greatly enhances the proliferation of naturally occurring HCV in HuS-E/2 cells. Similar results were also obtained for sera from additional patients (data not shown). To examine whether the infection is viral envelope-receptor mediated, the infection experiments using serum treated with anti-HCV-E2 antibody (α-E2) or with anti-tubulin (negative control) was also performed. Pre-incubation of the serum with α-E2 significantly reduced the total amount of HCV-RNA in the cells upon infection (Fig. 1B). This result suggested that the infection of natural HCV into 3D/TGP-HuS-E/2 cells was HCV-E2-dependent.

Inhibition of natural HCV replication in HuS-E/2 cells by Interferon

In order to test the effects of anti-viral agents on natural HCV replication in 3D/TGP HuS-E/2 cells, 50–100 U/ml of IFNα was added to the medium overlaying the HCV-RC5 infected 3D/TGP-HuS-E/2 cells. The two treatment concentrations resulted in the inhibition of HCV-RNA replication in 3D-HuS-E/2 cells by

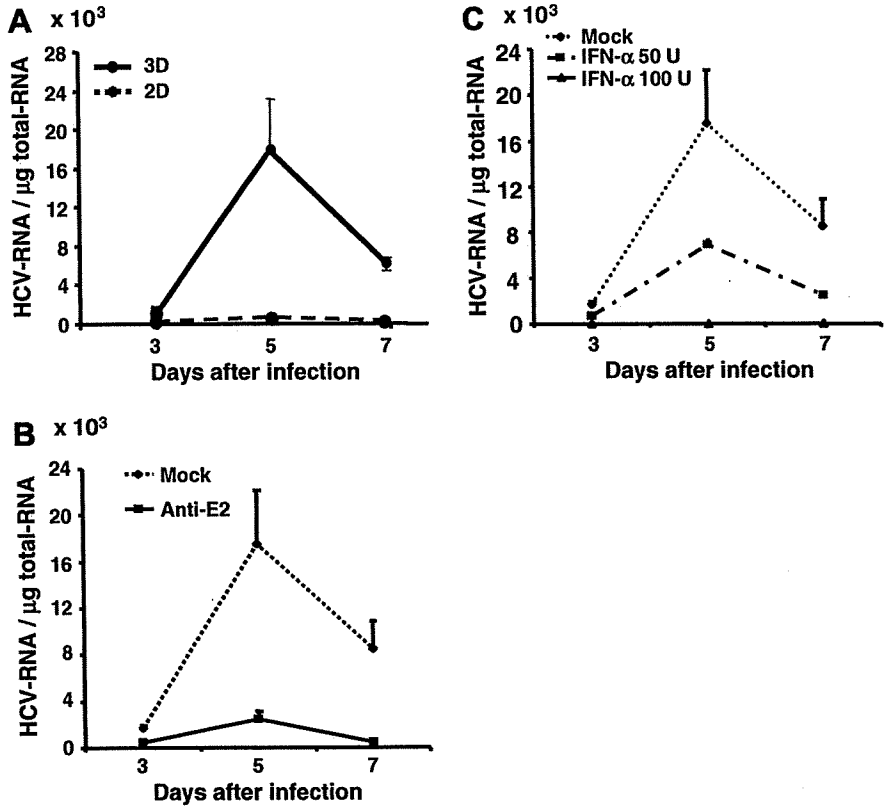

Fig. 1. HCV infection into 3D/TGP-HuS-E/2 cells. (A) 3D/TGP significantly enhanced HCV proliferation in HuS-E/2 cells. HCV patient serum was used to infect a similar number of HuS-E/2 cells cultured in 2D (hashed line) or 3D/TGP (solid line) culture for 24 h. Cells were then harvested and lysed at the indicated time points (3–7 days). The quantity of genomic HCV-RNA per 1 μg total RNA was determined by Q-PCR analysis. (B) Anti-E2 antibodies blocked HCV infection. HCV infection was performed as described in panel A in the presence of Anti-E2 specific or anti-tubulin (control) antibodies. (C) IFNα inhibits HCV replication in 3D/TGP-HuS-E/2 cells. HuS-E/2 cells were infected with HCV and fresh medium supplemented with or without (Mock), 50 U/ml, or 100 U/ml IFNα overlaid on the gel containing the cells and HCV proliferation measured as described above.

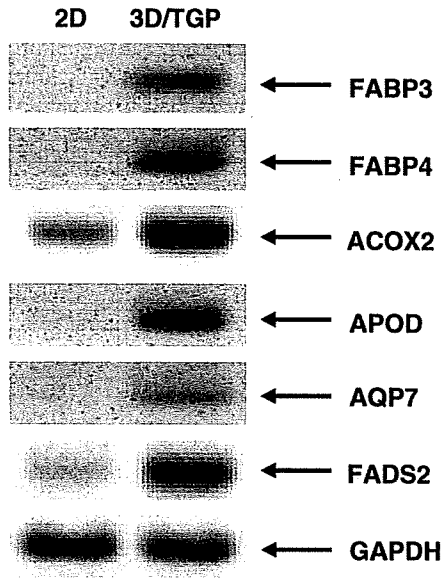

Fig. 2. RT-PCR analysis of the expression of genes identified by microarray. The PPARα regulated genes were increased in 3D/TGP-HuS-E/2 cells (3D-TGP) and their expression levels measured by RT-PCR. 2D represents RNA samples from 2D-HuS -E/2 cells. Twenty cycles of amplification were undertaken for the RT-PCR analysis. GAPDH expression served as an internal control. *Abbreviations:* FABP3, fatty acid binding proteins 3; FABP4, fatty acid binding proteins 4; ACOX2, acyl-coenzyme A oxidase 2; APOD, apolipoprotein D; AQP7, aquaporin 7; FADS2, fatty acid desaturase 2; GAPDH, glyceraldehyde 3-phosphate dehydrogenase.

approximately 50–60% and almost completely, respectively, when compared to the replication in cells receiving mock treatment (Fig. 1C). These results demonstrate that the IFNα treatment was effective on HCV derived from RC5 and that 3D/TGP-HuS-E/2 cells may be useful for the screening of anti-HCV drugs for the treatment of natural HCV.

Increased activation of the PPARα signaling pathway in 3D cultured HuS-E/2 cells

Given that 3D/TGP-HuS-E/2 cells demonstrated enhanced proliferation of natural HCV, the gene expression profiles of these cells was compared with that of cells cultured under normal 2D conditions using microarray analysis in order to identify the factors required for the enhanced proliferation. Among the 24,268 genes compared in this analysis, 212 genes demonstrated a greater than four folds index increase in expression in 3D/TGP than standard cultured cells. Cell signaling pathway analysis of these 212 genes showed that six genes, including fatty acid binding proteins 4 and 3 (FABP4 and 3), apolipoprotein D (APOD), aquaporin 7 (AQP7), acyl-coenzyme A oxidase 2 (ACOX2), and fatty acid desaturase 2 (FADS2), were targets of PPARα signaling [9–12]. The increased expression of these genes in the 3D/TGP-HuS-E/2 cells was further confirmed by RT-PCR analysis (Fig. 2). Given that PPARα is an essential factor for normal hepatocyte function [13], these results indicate that 3D/TGP culture enhances the hepatocyte-specific characteristics of HuS-E/2 cells.

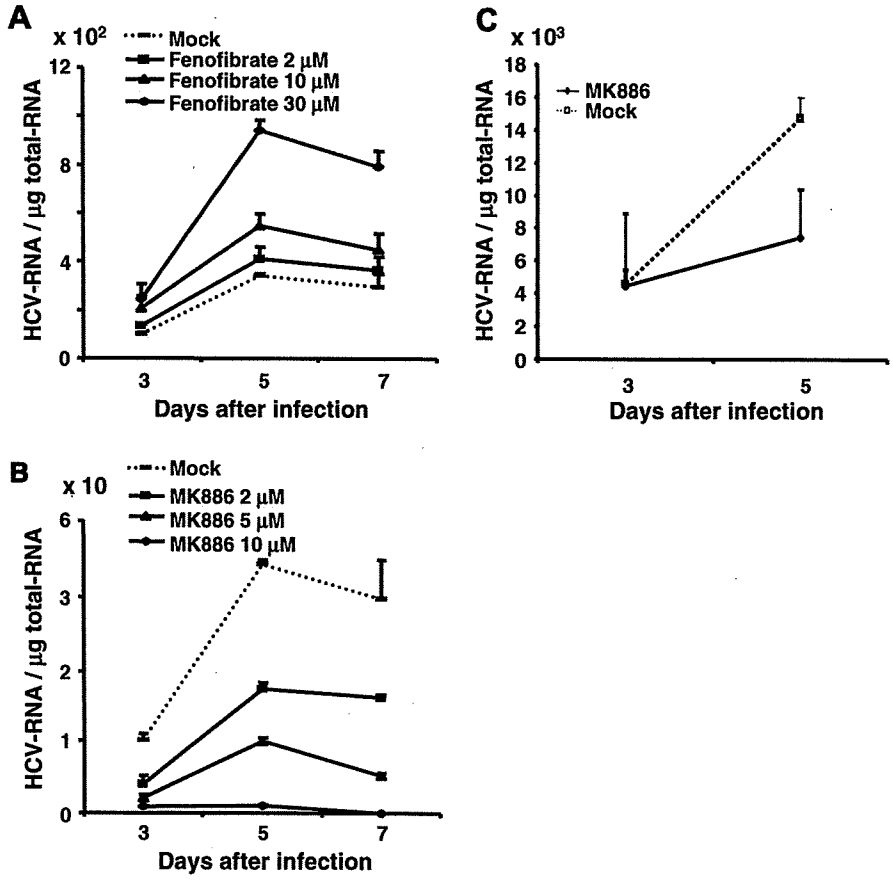

Fig. 3. The effects of PPARα agonists and antagonists on natural HCV proliferation. (A) HuS-E/2 cells were infected with HCV and fresh medium supplemented with or without (Mock) 2, 10, or 30 μM of fenofibrate overlaid on the cells. (B) Medium supplemented with or without (Mock), 2, 5, or 10 μM of MK886 was overlaid on 2D-HuS-E/2 cells infected with HCV. HCV proliferation following treatment was measured by Q-PCR. (C) Medium supplemented with or without (Mock), 10 μM of MK886 was overlaid on 3D/TGP-HuS-E/2 cells infected with HCV. HCV proliferation following treatment was measured by Q-PCR.

PPARα signaling affects HCV replication

We next examined the potential role of PPARα signaling on HCV proliferation by monitoring HCV replication in 2D-HuS-E/2 cells that had been infected with HCV-RC5 and subsequently treated with the PPARα agonist fenofibrate [14] or the PPARα antagonist MK886 [14] (Fig. 3B). As outlined in Fig. 3A, a dose-dependent increase in HCV replication was observed in fenofibrate-treated cells. In contrast, a dose-dependent decrease in HCV proliferation was observed in the presence of MK886. Similarly, treatment with MK886 reduced HCV proliferation in 3D/TGP-HuS-E/2 cells (Fig. 3C). The response of HCV proliferation in response to fenofibrate and MK886 treatment was also analyzed in LucNeo#2 cells that contained HCV replicon RNA (LNMH14) derived from the HCV-1b genome (Fig. 4A). Luciferase expression in these cells represented replication of the HCV replicon [6] and, as shown in Fig. 4A, luciferase activity in the cells treated with fenofibrate or MK886 also showed either enhancement or suppression of replicon proliferation, respectively. In addition, the increased HCV replication following fenofibrate treatment was completely abolished when treated with MK886 simultaneously. As MK886 is known to induce apoptosis when administered in high doses [15], the cell viability was examined using the XTT assay. There were no significant effects on cell viability after treatment with fenofibrate. Although MK886 resulted in a minor reduction in XTT values when high doses (10–15 μM) were administered, this reduction was not statistically significant when compared to its effect on HCV replication (Fig. 4B). This result suggests that PPARα signaling is required for HCV replication and that suppression of PPARα signaling has an anti-HCV effect.

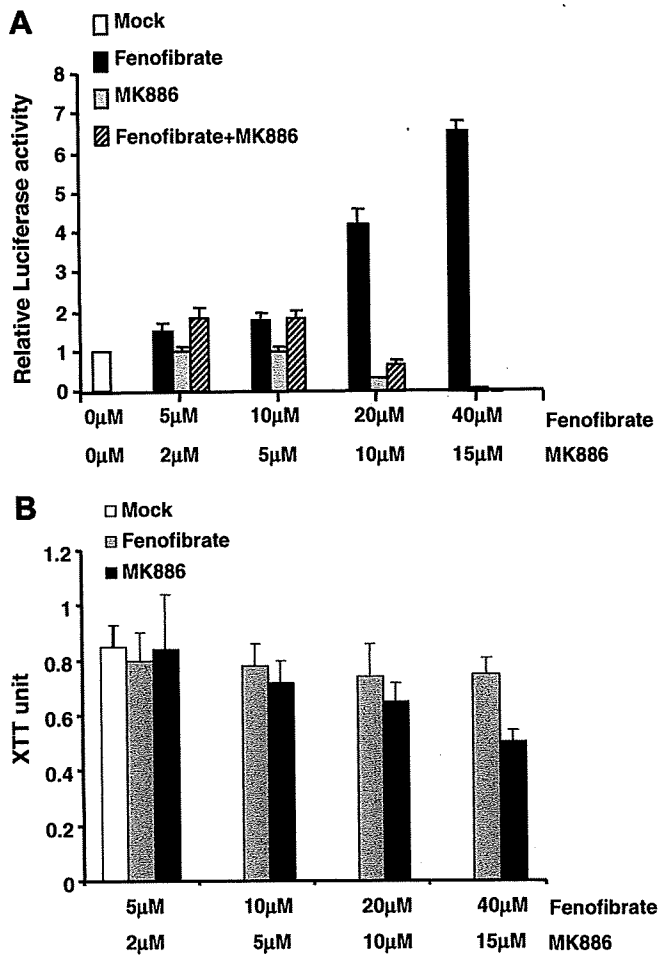

Fig. 4. The effects of PPARα agonists and antagonists on the replication of HCV subgenomic replicons. (A) LucNeo#2 cells containing a HCV subgenomic replicon termed LNMH14, were mock treated or treated with fenofibrate, MK886, or a combination of both fenofibrate and MK886 at the indicated concentrations for 2 days. Luciferase activity derived from the replicon was then measured as an indicator of HCV replication [7]. (B) Following treatment with fenofibrate and Mk886, LucNeo#2 cells were cultured for 2 days and cell viability measured using the XTT assay (Roche, Mannheim, Germany).

Discussion

In the current study, we demonstrated that immortalized hepatocyte HuS-E/2 cells cultured in 3D/TGP support the infection and replication of natural HCV derived from patient sera. Unlike recombinant HCVs, which have been required to adapt to sublines of HuH-7 cells [16], the population of the natural HCV is fairly polymorphic, demonstrating different responses to a variety of anti-viral agents [17,18]. The 3D/TGP-HuS-E/2 cells have the advantage of being a small-scale 3D cultured cells, which are cultured in 12-well plates at a density of 1×10^5/well, that allow the study of both viral and cellular events. In the current study, it demonstrated a 2 log increase in susceptibility to natural HCV infection and replication when compared to conventional 2D culture systems. Thus it offers an important advantage in the study of natural HCV infection and replication, and the response of natural HCV to anti-HCV drugs.

As the ability of HuS-E/2 cells to support infection and replication of natural HCV was greatly altered by the culture conditions, it is likely that the culture system described in our study will provide important information in regards to the cellular factors that support the HCV life cycle. The microarray study showed that the expression of some genes related to the PPARα signaling pathway were upregulated in the 3D cultured HuS-E/2 cells. Using both PPARα signaling agonists and antagonists, PPARα signaling was shown to affect infection and proliferation of natural HCV. PPARα is a ligand-activated transcription factor that is primarily expressed in tissues with high lipid metabolism including the liver, where it functions as one of three major nuclear receptors and is essential for its normal function [19]. Similar to a part of our data, a negative effect on HCV replication was previously observed in the replicon-bearing cells treated with siRNA for PPARα, with only 50% reduction of HCV-RNA [20]. In this study, even a large dose of PPARα agonist enhanced natural HCV replication in the 2D-HuS-E/2 cells for three times, despite the 2 logs enhancement of HCV proliferation in 3D/TGP culture. This implies that additional factors activated in 3D/TGP-HuS-E/2 cells may be required for the efficient HCV proliferation. Further analysis of the microarray data may provide us with further information on factors that may prove useful in the development of anti-HCV drugs.

In conclusion, the novel *in vitro* culture system combining TGP and immortalized hepatocytes described in this study demonstrated efficient support of natural HCV infection and replication. This system may be used in future virological studies to define new anti-HCV strategies. It may also prove useful for the specific design of effective individual therapy according to patient-specific strains.

Acknowledgments

This work was supported by Grants-in-Aid from the Ministry of Health, Labor and Welfare of Japan; and for scientific research from Ministry of Education, Sports, Culture, and Technology of Japan.

References

[1] Z. Younossi, J. Kallman, J. Kincaid, The effects of HCV infection and management on health-related quality of life, Hepatology 45 (2007) 806–816.

[2] M.W. Fried, M.L. Shiffman, K.R. Reddy, C. Smith, G. Marinos, F.L. Goncales Jr., D. Haussinger, M. Diago, G. Carosi, D. Dhumeaux, A. Craxi, A. Lin, J. Hoffman, J. Yu, Peginterferon alfa-2a plus ribavirin for chronic hepatitis C virus infection, N. Engl. J. Med. 347 (2002) 975–982.
[3] K. Murakami, K. Ishii, Y. Ishihara, S. Yoshizaki, K. Tanaka, Y. Gotoh, H. Aizaki, M. Kohara, H. Yoshioka, Y. Mori, N. Manabe, I. Shoji, T. Sata, R. Bartenschlager, Y. Matsuura, T. Miyamura, T. Suzuki, Production of infectious hepatitis C virus particles in three-dimensional cultures of the cell line carrying the genome-length dicistronic viral RNA of genotype 1b, Virology 351 (2006) 381–392.
[4] G. Andrei, Three-dimensional culture models for human viral diseases and antiviral drug development, Antiviral Res. 71 (2006) 96–107.
[5] H.H. Aly, K. Watashi, M. Hijikata, H. Kaneko, Y. Takada, H. Egawa, S. Uemoto, K. Shimotohno, Serum-derived hepatitis C virus infectivity in interferon regulatory factor-7-suppressed human primary hepatocytes, J. Hepatol. 46 (2007) 26–36.
[6] K. Goto, K. Watashi, T. Murata, T. Hishiki, M. Hijikata, K. Shimotohno, Evaluation of the anti-hepatitis C virus effects of cyclophilin inhibitors, cyclosporin A, and NIM811, Biochem. Biophys. Res. Commun. 343 (2006) 879–884.
[7] T. Murata, M. Hijikata, K. Shimotohno, Enhancement of internal ribosome entry site-mediated translation and replication of hepatitis C virus by PD98059, Virology 340 (2005) 105–115.
[8] M.A. El-Farrash, H.H. Aly, K. Watashi, M. Hijikata, H. Egawa, K. Shimotohno, In vitro infection of immortalized primary hepatocytes by HCV genotype 4a and inhibition of virus replication by cyclosporin, Microbiol. Immunol. 51 (2007) 127–133.
[9] J. Samulin, I. Berget, S. Lien, H. Sundvold, Differential gene expression of fatty acid binding proteins during porcine adipogenesis, Comp. Biochem. Physiol. B: Biochem. Mol. Biol. 151 (2008) 147–152.
[10] S. Hummasti, B.A. Laffitte, M.A. Watson, C. Galardi, L.C. Chao, L. Ramamurthy, J.T. Moore, P. Tontonoz, Liver X receptors are regulators of adipocyte gene expression but not differentiation: identification of apoD as a direct target, J. Lipid Res. 45 (2004) 616–625.
[11] C.G. Walker, M.J. Holness, G.F. Gibbons, M.C. Sugden, Fasting-induced increases in aquaporin 7 and adipose triglyceride lipase mRNA expression in adipose tissue are attenuated by peroxisome proliferator-activated receptor alpha deficiency, Int. J. Obes. (Lond.) 31 (2007) 1165–1171.
[12] D.G. Jump, D. Botolin, Y. Wang, J. Xu, B. Christian, O. Demeure, Fatty acid regulation of hepatic gene transcription, J. Nutr. 135 (2005) 2503–2506.
[13] D.W. Crabb, S. Liangpunsakul, Alcohol and lipid metabolism, J. Gastroenterol. Hepatol. 21 (Suppl. 3) (2006) S56–S60.
[14] D. Panigrahy, A. Kaipainen, S. Huang, C.E. Butterfield, C.M. Barnes, M. Fannon, A.M. Laforme, D.M. Chaponis, J. Folkman, M.W. Kieran, PPARalpha agonist fenofibrate suppresses tumor growth through direct and indirect angiogenesis inhibition, Proc. Natl. Acad. Sci. USA 105 (2008) 985–990.
[15] V.S. Deshpande, J.P. Kehrer, Mechanisms of *N*-acetylcysteine-driven enhancement of MK886-induced apoptosis, Cell Biol. Toxicol. 22 (2006) 303–311.
[16] K.J. Blight, A.A. Kolykhalov, C.M. Rice, Efficient initiation of HCV RNA replication in cell culture, Science 290 (2000) 1972–1974.
[17] R.C. Dickson, Clinical manifestations of hepatitis C, Clin. Liver Dis. 1 (1997) 569–585.
[18] E.J. Heathcote, Antiviral therapy: chronic hepatitis C, J. Viral Hepat. 14 (Suppl. 1) (2007) 82–88.
[19] C.N. Palmer, M.H. Hsu, K.J. Griffin, J.L. Raucy, E.F. Johnson, Peroxisome proliferator activated receptor-alpha expression in human liver, Mol. Pharmacol. 53 (1998) 14–22.
[20] B. Rakic, S.M. Sagan, M. Noestheden, S. Belanger, X. Nan, C.L. Evans, X.S. Xie, J.P. Pezacki, Peroxisome proliferator-activated receptor alpha antagonism inhibits hepatitis C virus replication, Chem. Biol. 13 (2006) 23–30.

JOURNAL OF VIROLOGY, Jan. 2010, p. 303–311
0022-538X/10/$12.00 doi:10.1128/JVI.01448-09
Copyright © 2010, American Society for Microbiology. All Rights Reserved.
Vol. 84, No. 1

Pathogenesis of Hepatitis C Virus Infection in *Tupaia belangeri*▽†

Yutaka Amako,[1] Kyoko Tsukiyama-Kohara,[1,2] Asao Katsume,[1,3] Yuichi Hirata,[1] Satoshi Sekiguchi,[1] Yoshimi Tobita,[1] Yukiko Hayashi,[4] Tsunekazu Hishima,[4] Nobuaki Funata,[4] Hiromichi Yonekawa,[5] and Michinori Kohara[1]*

Department of Microbiology and Cell Biology, Tokyo Metropolitan Institute of Medical Science, 2-1-6, Kamikitazawa, Setagaya-ku, Tokyo 156-0057, Japan[1]; Department of Experimental Phylaxiology, Faculty of Medical and Pharmaceutical Sciences, Kumamoto University, 1-1-1 Honjo Kumamoto City, Kumamoto 860-8556, Japan[2]; Fuji Gotemba Research Laboratory, Chugai Pharmaceutical Company, Ltd., 135, Komakado 1 Chome, Gotemba-shi, Shizuoka 412-8513, Japan[3]; Department of Pathology, Tokyo Metropolitan Komagome Hospital, 3-18-22 Honkomagome, Bunkyo-ku, Tokyo 113-8677, Japan[4]; and Laboratory of Animal Science, Tokyo Metropolitan Institute of Medical Science, 2-1-6, Kamikitazawa, Setagaya-ku, Tokyo 156-0057, Japan[5]

Received 14 July 2009/Accepted 5 October 2009

The lack of a small-animal model has hampered the analysis of hepatitis C virus (HCV) pathogenesis. The tupaia (*Tupaia belangeri*), a tree shrew, has shown susceptibility to HCV infection and has been considered a possible candidate for a small experimental model of HCV infection. However, a longitudinal analysis of HCV-infected tupaias has yet to be described. Here, we provide an analysis of HCV pathogenesis during the course of infection in tupaias over a 3-year period. The animals were inoculated with hepatitis C patient serum HCR6 or viral particles reconstituted from full-length cDNA. In either case, inoculation caused mild hepatitis and intermittent viremia during the acute phase of infection. Histological analysis of infected livers revealed that HCV caused chronic hepatitis that worsened in a time-dependent manner. Liver steatosis, cirrhotic nodules, and accompanying tumorigenesis were also detected. To examine whether infectious virus particles were produced in tupaia livers, naive animals were inoculated with sera from HCV-infected tupaias, which had been confirmed positive for HCV RNA. As a result, the recipient animals also displayed mild hepatitis and intermittent viremia. Quasispecies were also observed in the NS5A region, signaling phylogenic lineage from the original inoculating sequence. Taken together, these data suggest that the tupaia is a practical animal model for experimental studies of HCV infection.

Hepatitis C virus (HCV) is a small enveloped virus that causes chronic hepatitis worldwide (32). HCV belongs to the genus *Hepacivirus* of the family *Flaviviridae*. Its genome comprises 9.6 kb of single-stranded RNA of positive polarity flanked by highly conserved untranslated regions at both the 5′ and 3′ ends (4, 27, 29). The 5′ untranslated region harbors an internal ribosomal entry site (29) that initiates translation of a single open reading frame encoding a large polyprotein comprising about 3,010 amino acids (35). The encoded polyprotein is co- and posttranslationally processed into 10 individual viral proteins (15).

In most cases of human infection, HCV is highly potent and establishes lifelong persistent infection, which progressively leads to chronic hepatitis, liver steatosis, cirrhosis, and hepatocellular carcinoma (9, 16, 21). The most effective therapy for treatment of HCV infection is administration of pegylated interferon combined with ribavirin. However, the combination therapy is an arduous regimen for patients; furthermore, HCV genotype 1b does not respond efficiently (19). The prevailing scientific opinion is that a more viable option than interferon treatment is needed.

The chimpanzee is the only validated animal model for in vivo studies of HCV infection, and it is capable of reproducing most aspects of human infection (5, 18, 23, 28, 35, 36). The chimpanzee is also the only validated animal for testing the authenticity and infectivity of cloned viral sequences (8, 14, 35, 36). However, chimpanzees are relatively rare and expensive experimental subjects. Cross-species transmission from infected chimpanzees to other nonhuman primates has been tested but has proven unsuccessful for all species evaluated (1).

The tupaia (*Tupaia belangeri*), a tree shrew, is a small nonprimate mammal indigenous to certain areas of Southeast Asia (6). It is susceptible to infection with a wide range of human-pathogenic viruses, including hepatitis B viruses (13, 20, 31), and appears to be permissive for HCV infection (33, 34). In an initial report, approximately one-third of inoculated animals exhibited acute, transient infection, although none developed the high-titer sustained viremia characteristic of infection in humans and chimpanzees (33). The short duration of follow-up precluded any observation of liver pathology. In addition to the putative in vivo model, cultured primary hepatocytes from tupaias can be infected with HCV, leading to de novo synthesis of HCV RNA (37). These reports strongly support tupaias as a valid model for experimental studies of HCV infection. However, longitudinal analyses evaluating the clinical development and pathology of HCV-infected tupaias have yet to be exam-

* Corresponding author. Mailing address: Department of Microbiology and Cell Biology, The Tokyo Metropolitan Institute of Medical Science, 2-1-6, Kamikitazawa, Setagaya-ku, Tokyo 156-0057, Japan. Phone: 81-3-5316-3232. Fax: 81-3-5316-3137. E-mail: kohara-mc@igakuken.or.jp.

† Supplemental material for this article may be found at http://jvi.asm.org/.

▽ Published ahead of print on 21 October 2009.

TABLE 1. Experimental HCV infections performed in this study

Tupaia no.	Inoculum		Biopsy/sacrifice[b]
	Type	Quantity (GE/tupaia)[a]	
Group I[c]			
Tup.4	RCV	1×10^7	84, 94/144 wk p.i.
Tup.5	HCR6	6×10^5	95, 105/155 wk p.i.
Tup.6	HCR6	6×10^5	95, 105/155 wk p.i.
Tup.8	RCV	1×10^7	84, 94/144 wk p.i.
Group II[d]			
Tup.9	Tup.5 (5 wk p.i.)	1×10^2	NT
Tup.10	Tup.5 (5 wk p.i.)	1×10^2	NT
Tup.11	Tup.8 (10 wk p.i.)	1×10^2	NT
Tup.12	Tup.8 (10 wk p.i.)	1×10^2	NT
Tup.13	Tup.4 (8 wk p.i.)	1×10^2	NT
Tup.14	Tup.4 (8 wk p.i.)	1×10^2	NT
Group III[e]			
Tup.15	None		92/100 wk
Tup.17	None		92/100 wk
Tup.38	None		242 wk
Tup.39	None		242 wk

[a] Viral RNA GE/tupaia was estimated by Quantitative real-time RT-PCR (GE, genome equivalents; sensitivity > 10 GE/ml serum).
[b] Liver biopsy was performed at indicated time-point. p.i., postinoculation; NT, not tested.
[c] Group I, primary infection experiment in which 1-year-old animals were inoculated with two different types of inocula.
[d] Group II, reinfection experiment, where HCV RNA-positive sera from Group I experimental infections were passaged to naive animals.
[e] GroupIII, no-infection control.

ined. In the present study, we describe the clinical development and pathology of HCV-infected tupaias over an approximately 3-year time course.

MATERIALS AND METHODS

Animals. Table 1 summarizes the tupaias used in this study. Tupaias born in laboratory captivity were obtained from the Laboratory Animal Center at the Kunming Institute of Zoology (Chinese Academy of Sciences). Tupaias were imported with permission from the Convention on International Trade in Endangered Species of Wild Fauna and Flora (7), quarantined for medical inspection, and housed individually in standard rat cages supplied with filtered air. The animals were fed a daily regimen of eggs, fruit, and the CMS-1 commercial diet for marmosets (CLEA, Japan). Their appetites and feces were carefully monitored. Animal care and experimental handling conformed to study guidelines established by the Subcommittee on Laboratory Animal Care at the Tokyo Metropolitan Institute of Science.

Patient serum used for animal infection. HCV genotype 1b serum, designated HCR6, was obtained from a patient with chronic active hepatitis C. The infectious titer of HCR6 was determined in chimpanzee and Molt4 cells and denoted plasma K (HCR6) by Shimizu et al. (24). The HCR6 serum exhibited a PCR titer of 6×10^6 genome equivalents/ml and an infectious titer of 3.7×10^4 50% chimpanzee infectious doses/ml. Serum aliquots were frozen at −80°C until they were used.

Virion reconstitution of cloned HCV. As described previously, pHCR6 (genotype 1b; 9,611 nucleotides; GenBank accession no. AY045720) is a plasmid carrying HCV genomic cDNA cloned from HCR6 serum (30). pHCR6Rz was designed for precisely trimmed RNA expression, with the entire genomic region of pHCR6Rz recloned under the control of the T7 promoter and the 5′ and 3′ distal ends flanked by hammerhead- and hepatitis D virus ribozyme-encoding sequences, respectively (22, 25).

For molecular reconstitution of HCV particles, pHCR6Rz was transfected into IMY-N9 cells as described previously (12). Briefly, semiconfluent IMY-N9 cells in 100-mm plastic dishes were transfected with 15 μg of plasmid using 40 μl of cationic lipids (DMRIE-C reagent; Life Technology) in accordance with the manufacturer's instructions. Five hours after transfection, the cells were infected with AdexCAT7 (2) (kindly provided by Y. Matsuura) at a multiplicity of infection of 20. After infection, the culture medium was replaced with Hepato-STIM (Becton Dickinson). The culture supernatants were collected at 24 h postinfection and stored at −80°C.

Virus inoculation and collection of serum samples. Animals were infected at 6 months of age. The anesthetic agent, ketamine hydrochloride, was administered intramuscularly at 50 mg/kg body weight prior to virus inoculation and bleeding of the tupaias. The inocula were introduced intravenously at 6×10^5 genome equivalents/animal for patient serum HCR6 and 1×10^7 genome equivalents/animal for reconstituted virions derived from the pHCR6Rz inoculation. Blood samples were drawn from infected and control animals pre- and postinfection. Briefly, the animals were bled weekly for 20 weeks and biweekly thereafter. At each time point, 0.5 ml of blood was drawn from the thigh vein; the sera were separated, aliquoted, and stored for subsequent assays.

Reinfection experiments were performed by transmission of HCV RNA-positive serum from group I (Table 1) to naive animals.

Serum alanine aminotransferase (ALT) concentrations were determined using a Transnase Nissui kit (Nissui Pharmaceutical Co.), standardized, and displayed as IU/liter.

RNA isolation and quantitative RTD-PCR assay for HCV RNA. Serum samples (100 μl) were tested for circulating HCV RNA in vivo using quantitative real-time detection (RTD)-PCR (TaqMan). RNA was extracted from the sera and livers of sacrificed animals using the acid guanidium-phenol chloroform method with tRNA as a carrier (3). Two tupaias (Tup.5 and Tup.6) were inoculated with patient serum HCR6. Another two animals (Tup.4 and Tup.8) were inoculated with reconstituted viral particles (RCV). Tup.15 served as a mock-infected control. Liver specimens (3- to 4-mm^2 blocks) from these tupaias were homogenized with 1.5 ml of 5 M guanidine thiocyanate using a polytron-type homogenizer (Ultra-Turrax T25; IKA Laborteehnik, Staufen, Germany). RNA was then reextracted with 4 M guanidine thiocyanate.

RNA samples were subjected to RTD-PCR on an ABI 7700 sequence detector (Applied Biosystems) as described previously (26). The extracted RNA was dissolved in 200 μl of diethyl pyrocarbonate-treated water containing 10 mM dithiothreitol and 200 units/ml RNase inhibitor in a siliconized tube. RTD-PCR was performed using 1 μg of total RNA, one set of PCR primers, and a probe for a location within the 5′ noncoding region using the EZ *rTth* RNA PCR kit (Perkin Elmer) and the ABI Prism 7700 sequence detector system. A standard curve was constructed using a 10-fold dilution series of in vitro-transcribed and previously titrated synthetic HCV RNA.

Consequently, the quantities represented by genome equivalents correspond to an absolute standard curve (26). All quantitative RTD-PCR assays were performed using duplicate samples, with both negative control serum and HCV-positive serum included. The control sera were diluted before use and were estimated to contain low copy numbers of HCV RNA (100 genome equivalents/ml serum). Samples were deemed positive for HCV RNA if both duplicates yielded PCR-amplified product. Averages of the two estimated values are shown in the figures.

Histological analysis. Tissue samples were carefully collected from anesthetized animals by abdominal incision, fixed in 10% neutral buffered formalin, embedded in paraffin, sectioned, and stained with hematoxylin and eosin (H&E). Silver and Sudan IV (Wako Pure Chemical Industries, Ltd.) staining were also carried out to visualize fiber generation and lipid degeneration, respectively. All histological staining was performed in accordance with conventional procedures. The histological status was determined using the modified hepatitis activity index scoring system, which grades necrosis and inflammation on a scale of 0 to 18 (periportal inflammation and necrosis, 0 to 10; lobular inflammation and necrosis, 0 to 4; portal inflammation, 0 to 4) (11). Fibrosis was scored using the Ishak fibrosis scale of 0 to 6 (0, no fibrosis; 1 or 2, portal fibrosis; 3 or 4, bridging fibrosis; and 5 or 6, cirrhosis). The values in each group (Table 2) represent the averages of the scores in five visual fields.

Statistical analysis. The statistical significance of differences between controls and HCV-infected animals was analyzed with the nonparametric Mann-Whitney U test. All comparisons were two tailed. The statistical analysis was conducted with SPSS 12.0 software (SPSS Inc., Chicago, IL).

RESULTS

Inoculation of HCV causes acute hepatitis and transient viremia in tupaias. To begin this study, two distinct but related inocula were chosen for infection of tupaias. Serum from a chronic hepatitis patient (designated HCR6) was chosen for its

TABLE 2. Grading: necroinflammatory scores and fibrosis

Group	Inoculum	Tupaia no.	Grade				Total	Avg	SD	Staging
			A	B	C	D				
94 wk p.i. (biopsy)										
I	HCR 6	Tup.5	0	0	0	0	0	1.3	1.5	0
		Tup.6	1	0	1	0	2			0
	RCV	Tup.4	0	0	0	0	0			0
		Tup.8	0	0	0	3	3			6
	Control	Tup.15	0	0	0	0	0	0	0	0
III		Tup.17	0	0	0	0	0			0
		Tup.38								
		Tup.39								
144 wk p.i. (sacrifice)										
I	HCR 6	Tup.5	1	0	2	3	6	5.5	3.7	0
		Tup.6	3	0	4	3	10			1
	RCV	Tup.4	0	0	0	1	1			0
		Tup.8	1	0	1	3	5			6
	Control	Tup.15						0	0	
III		Tup.17								
		Tup.38	0	0	0	0	0			0
		Tup.39	0	0	0	0	0			0

defined genotype (genotype 1b), and genetic heterogeneity was ascertained by the process of cloning consensus cDNA. The infectivity of this serum was also experimentally defined in chimpanzees; a 50% chimpanzee infectious dose was estimated at 3.7×10^4 50% chimpanzee infectious doses/ml. Furthermore, the consensus genomic sequence of HCV was cloned from the serum (pHCR6; 9,611 bases; GenBank AY045702.1). For the second inoculum (referred to as RCV), clonal viral particles were reconstituted as described in Materials and Methods. This inoculum was expected to be free of neutralizing antibodies and thus was considered potentially more infectious than patient sera. In the case of RCV infection, genetic diversification of viral RNA, also known as quasispecies, can be regarded as a direct indication of de novo synthesis of progenitor virus in vivo.

Either patient serum or cDNA-derived RCV was inoculated into tupaias (Table 1, group I). Two animals (one female and one male) were tested against each inoculum. Age-matched animals were bred as infection-free controls.

All experimental infections are described in Materials and Methods and Table 1. Prior to experimental infection, the normal serum ALT level in tupaias was measured at 22.3 IU/liter ($n = 23$).

Inoculation with patient serum HCR6 caused rapid fluctuations in the serum ALT concentrations, from two- to fivefold, in both inoculated tupaias, suggesting acute hepatitis in vivo (Fig. 1A and B). Correlative quantitative RTD-PCR revealed HCV viremia soon after serum inoculation in Tup.5, which continued to show transient viremia long term. The appearance of viremia sometimes coincided with a steep elevation in the serum ALT (Fig. 1A). Conversely, HCV RNA was not detected in the serum of Tup.6 up to 60 weeks postinoculation and only twice thereafter. Acute-phase ALT elevations (3 to 4 weeks postinoculation) in Tup.6 might represent tight control of HCV infection by the host immune system (Fig. 1B).

Distinct results were obtained for the two animals (Tup.4 and Tup.8) inoculated with RCV. Both animals displayed sustained viremia up to 10 weeks postinoculation (Fig. 1C and D), indicating persistent HCV infection and inability to eradicate the virus. Viremia was detected intermittently throughout the course of infection, sometimes accompanying the elevation of serum ALT. Humoral immune responses in Tup.5 and Tup.6 (see Fig. S1A in the supplemental material) and Tup.4 and Tup.6 (see Fig. S1B in the supplemental material) were indicated.

We performed RTD-PCR to confirm whether HCV could replicate in the tupaias' livers (Tup.4, Tup.5, Tup.6, and Tup.8) and obtained the following results (Fig. 1E): 310 ± 117 copies/μg total RNA in Tup.5, 80 ± 11 copies/μg in Tup.6, 199 ± 77 copies/μg in Tup.4, and 292 ± 48 copies/μg in Tup.8. In contrast, HCV RNA was not detected in the liver of the mock-infected animal (Tup.15).

HCV RNA was also not detected in samples from either preinoculation or age-matched, infection-free control tupaias (Table 1, group III), nor were significant elevations in serum ALT observed for any of the three infection-free controls (data not shown).

HCV causes chronic hepatitis in tupaia liver, leading to fibrosis and cirrhosis. Serum ALT and circulating HCV RNA levels in primary infected tupaias (Table 1, group I) were monitored for 3 years postinoculation. As described above, the magnitudes of serum ALT fluctuations varied substantially among infected animals (Fig. 1A, B, C, and D). Tupaia livers were examined for histological lesions in order to elucidate if HCV caused chronic hepatitis. Liver biopsies via abdominal incisions were performed at 2 years postinoculation. All animals were sacrificed at 3 years postinoculation (4.5 years for uninfected animals). H&E staining of liver specimens from HCV-infected tupaias showed infiltrating lymphocytes within sinusoids and around portal areas, indicating chronic hepatitis in the tupaia livers (Fig. 2B, D, and H). Infiltrating lymphocytes were also observed in limiting plates, indicating ongoing inflammation (Fig. 2G and H). Furthermore, a comparison of liver samples at 2 and 3 years postinoculation revealed that the

Downloaded from jvi.asm.org at KUMAMOTO UNIVERSITY on December 15, 2009

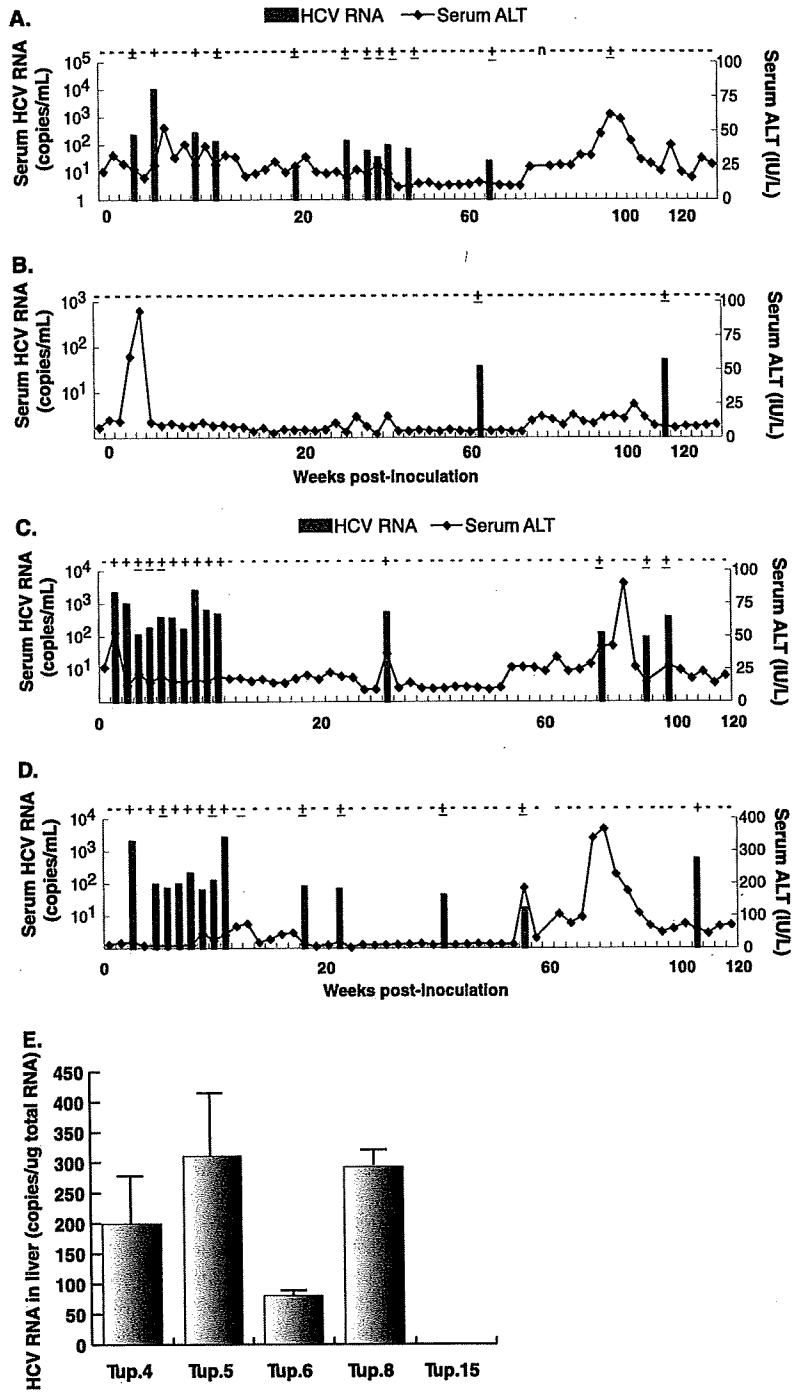

FIG. 1. Course of infection with patient serum HCR6 and RCV. (A) The results of quantitative RTD-PCR for HCV RNA and serum ALT concentrations were combined and plotted to show the course of infection in Tup.5. The bars and the ordinates on the left represent HCV RNA as genome equivalents/ml of serum. The curved line and the ordinates on the right represent serum ALT concentrations as IU/liter serum. (B) Serum HCV RNA and ALT concentrations for infection of Tup.6. (C) The graph for Tup.4. (D) The graph for Tup.8. The vertical axis for serum ALT in this graph is scaled differently from the others because of significant ALT elevation. (E) Quantification of HCV RNA in tupaia liver. HCV RNA in hepatocytes from tupaia (Tup.4, Tup.5, Tup.6, Tup.8, and Tup.15) livers was isolated 172 weeks after HCV infection and quantified by RTD-PCR. As few as 10 copies of the genome were detected, and the quantification range was between 10^1 and 10^8 copies (26).

Downloaded from jvi.asm.org at KUMAMOTO UNIVERSITY on December 15, 2009

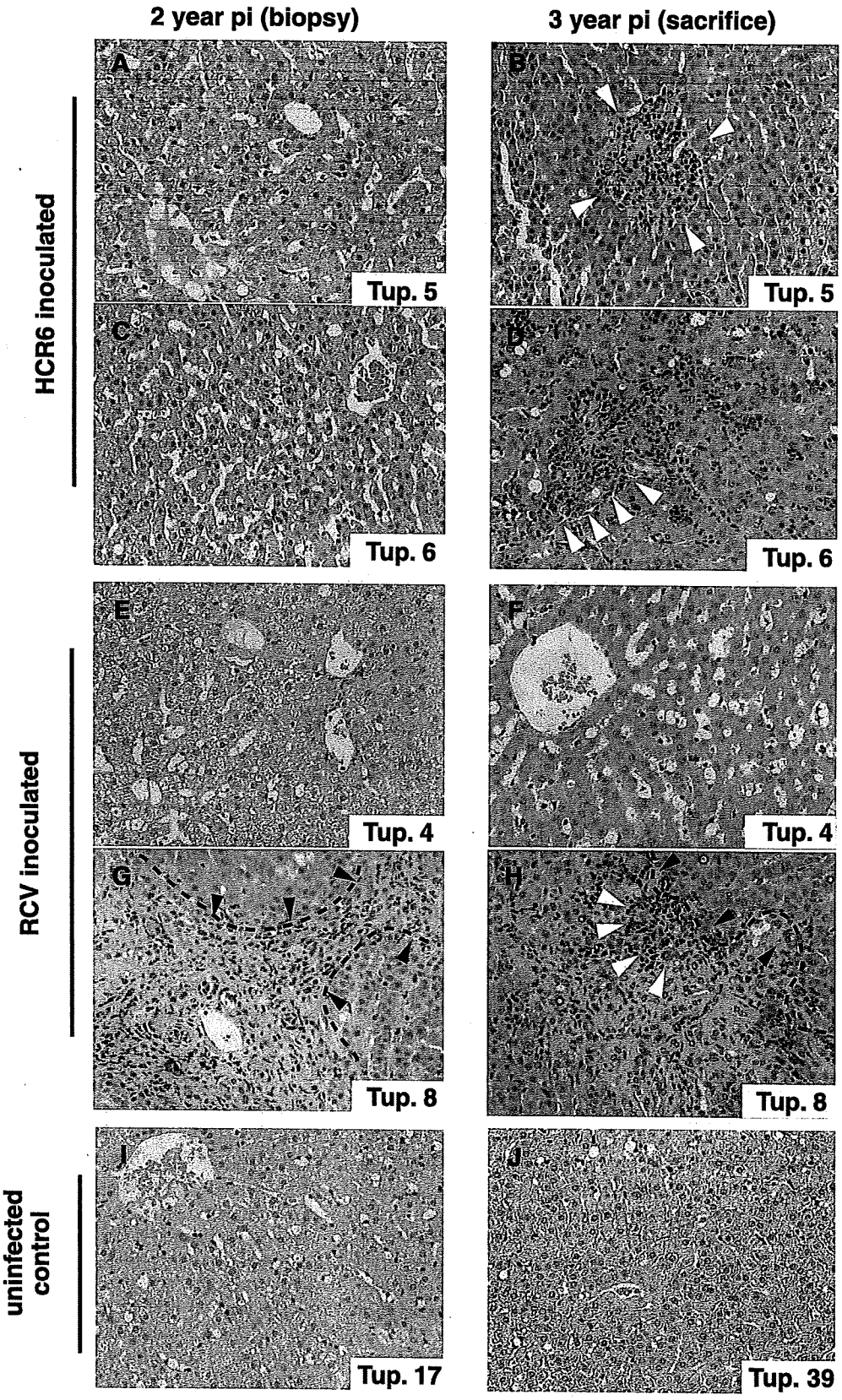

FIG. 2. Micrographs of liver specimens stained with H&E. Liver tissue from HCR6-inoculated tupaias (A to D) and RCV-inoculated tupaias (E to H) was obtained at 2 and 3 years postinoculation (pi). (I and J) Liver specimens from uninfected animals age matched to each inoculated animal were also obtained. The HCV-infected tupaia livers harbored infiltrating lymphocytes (white arrowheads) and fibrosis (broken lines and black arrowheads), which indicate chronic hepatitis.

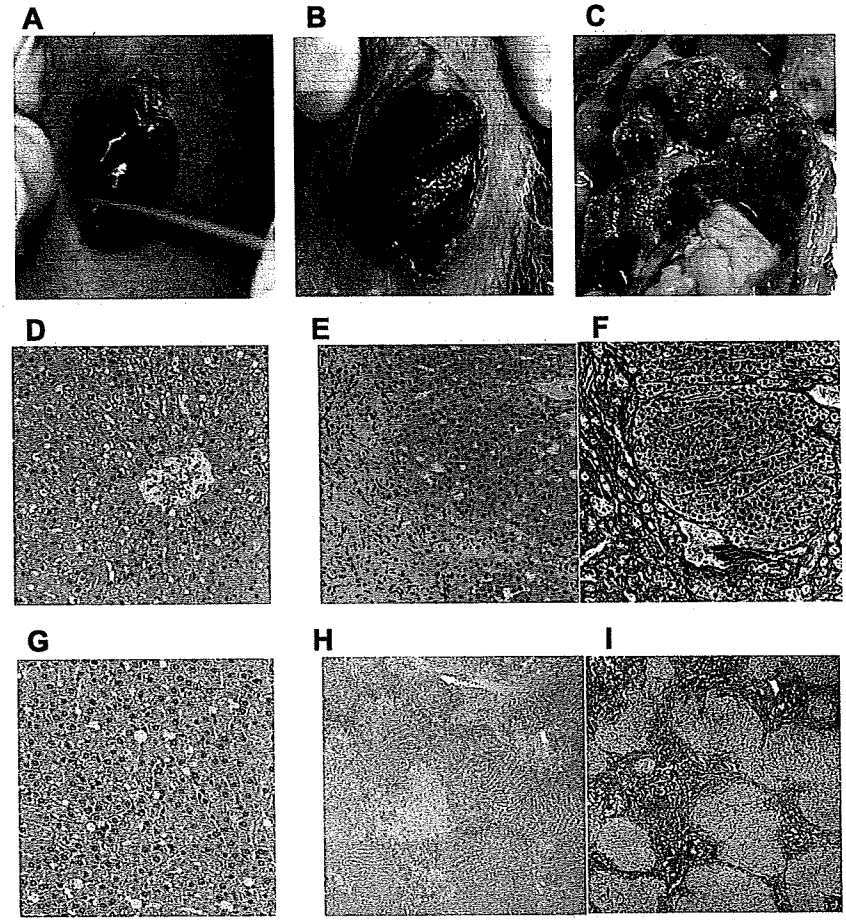

FIG. 3. Macro- and microscopic features of tupaia liver. (A) Infection-free control tupaia (Tup.15; 92 weeks). (B) RCV-infected animal displaying liver cirrhosis (Tup.8; 84 weeks postinoculation). (C) RCV-infected animal with massive surface nodules (Tup.8; 144 weeks postinoculation). (D and G) H&E staining of the uninfected Tup.15 at 92 weeks (D) and the uninfected Tup.39 at 242 weeks (G). (E, F, H, and I) H&E and silver staining of Tup.8 at 84 weeks postinoculation (E and F) or at 144 weeks postinoculation (H and I).

hepatitis had worsened with time in all HCV-infected tupaias (Fig. 2A to H and Table 2).

Fibrosis and cirrhosis were also examined. Mild fibrosis was seen in Tup.6, while severe fibrosis was seen in Tup.8. Cirrhosis was histologically investigated in all animals (Table 2). There was no significant difference between groups I and III at 94 weeks postinfection ($P = 0.194$), but at 144 weeks postinfection, a slight difference was observed ($P = 0.059$; SPSS 12.0). Macroscopic observation of the liver biopsy specimens (taken 2 years postinoculation) indicated liver cirrhosis in Tup.8 (Fig. 3B) compared with Tup.15 (uninfected control) (Fig. 3A), while silver staining of histology samples revealed fibrosis and cirrhotic nodules (Fig. 3E and F). Macroscopic observation upon sacrifice (3 years postinoculation) indicated that liver cirrhosis in Tup.8 had worsened (Fig. 3C). In contrast, age-matched infection-free negative control tupaias displayed none of these pathologies (Fig. 3A, D, and G).

Progressive lipid degeneration was noted in infected tupaias throughout the course of infection (Fig. 4). In particular, Tup.5 displayed microvesicular lipid droplets in the first biopsy specimens (at 2 years), which developed into macrovesicular droplets and foamy degeneration in biopsy specimens at 3 years (Fig. 4C and D). Liver specimens from other infected animals displayed intracellular micro- and macrovesicular lipid droplets in hepatocytes at 3 years postinoculation (Fig. 4F, H, and J). These anomalies were not present in liver specimens from infection-free control animals (Fig. 4A and B).

Transmission of viral-RNA-positive serum to naive animals reproduces acute hepatitis and viremia. To confirm virion regeneration in vivo, and to exclude the possibility of false-positive serum HCV RNA results due to amplification of the original inocula, HCV RNA-positive sera from primary inoculated tupaias were used to inoculate naive tupaias. Three different sera were tested in this passage experiment, with two naive tupaias used as recipient animals for each trial (see Materials and Methods) (Table 1, group II).

In the first reinfection experiment, serum from Tup.5 (originally infected with patient serum HCR6) was collected at 5 weeks postinoculation and used to infect two naive animals. The recipient animals showed intermittent viremia over the subsequent 3 months (Fig. 5A). In the second and third cases of reinfection, sera from Tup.8 at 10 weeks postinoculation and from Tup.4 at 8 weeks postinoculation also induced viremia in the naive inoculated animals, similar to the first reinfection experiment (Fig. 5B and C). Furthermore, the PCR titers of the recipient tupaias were significantly greater than the inoc-

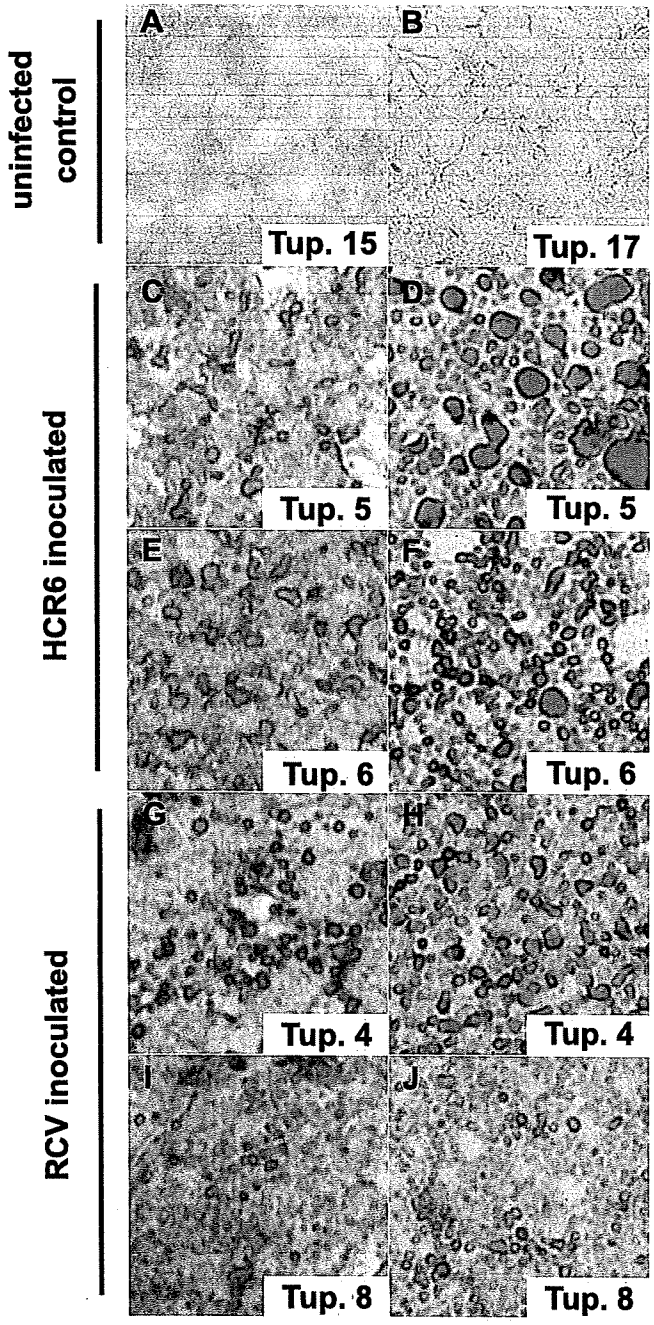

FIG. 4. Sudan IV-stained liver specimens exhibiting fatty liver degeneration. Cryosections of liver stained by Sudan IV as described in Materials and Methods show fatty liver degeneration. The left and right columns display biopsy specimens of infected animals (2 years postinoculation) and animals sacrificed at 3 years postinfection, respectively. (A and B) Uninfected controls at 2 years (Table 1 shows sample timing). (C to F) Patient serum HCR6-infected animals. (G to J) RCV-infected animals.

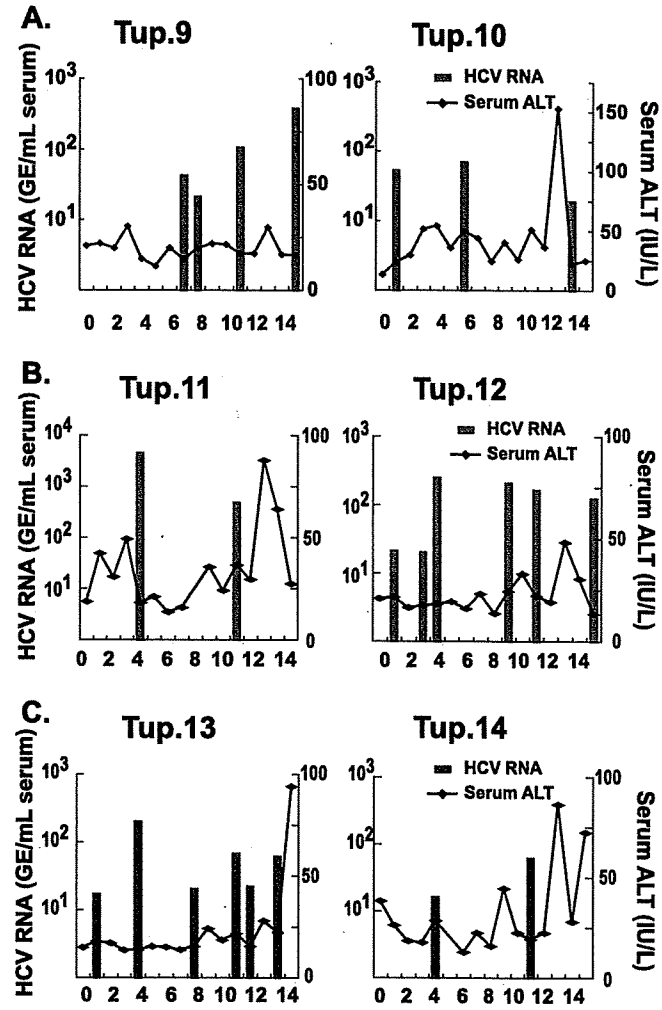

FIG. 5. Results of a reinfection experiment. (A) Quantitative RTD-PCR for HCV RNA and serum ALT levels are shown. Two naive animals were inoculated with tupaia serum (using serum taken at 5 weeks postinoculation from Tup.5, originally inoculated with patient serum HCR6) containing 100 genome equivalents (GE)/ml and were monitored for 15 weeks postinoculation (Table 1). (B) Tupaia serum (taken at 10 weeks postinoculation from Tup.8, originally inoculated with RCV) that was positive for HCV RNA was passaged into two naive animals. The animals were inoculated with tupaia serum at 100 GE/animal and monitored for 15 weeks postinoculation. (C) Tupaia serum (taken at 8 weeks postinoculation from Tup.4, originally inoculated with RCV) that was positive for HCV RNA was passaged into naive animals. The animals were inoculated with serum at 100 GE/animal and monitored for 20 weeks postinoculation.

ulation titers (10^2 genome equivalents/animal) (Table 1). For Tup.11, serum from 4 weeks postinoculation contained almost 10^4 genome equivalents/ml of HCV RNA (Fig. 5B). In addition, significant increases in serum ALT accompanied detection of serum HCV RNA. These results indicate that HCV RNA-positive sera from group I actually contained infectious virion particles. They also suggest that reconstituted HCV particles made from cDNA are infectious in tupaias.

We amplified a portion of the NS5A sequence, which is known as the interferon sensitivity determining region, by reverse transcription-PCR as described in the supplemental material. Each PCR product was subcloned and sequenced to compare the encoded amino acid sequences. For the purposes of this study, animals were inoculated with a molecular clonal virus consisting of a unique viral sequence of cDNA. The interferon sensitivity determining region sequences recovered from an animal infected with clonal inoculum (Tup.8 at 103 weeks postinoculation) were found to be heterogeneous, with

a few amino acid substitutions (K2212M for 2/10 cases, L2232P for 1/10 cases, and L2253S for 6/10 cases) (see Fig. S2E in the supplemental material). Interestingly, the codon for amino acid 2224 encodes valine, but it was found to be variant for alanine and valine in sequences from the original patient serum (HCR6). Tupaias infected with patient serum also exhibited variability at position 2224; valine occupancy was rare, as was seen in the original HCR6 population (see Fig. S2B and C in the supplemental material). On the other hand, this position was occupied solely by valine for sequences recovered from Tup.8 (see Fig. S2E in the supplemental material), indicating that genetic variations shown for Tup.8 originated from the pHCR6 cDNA sequence. Taken together, quasispecies detection of circulating virus represents further evidence demonstrating intrinsic replication of HCV in tupaias despite low levels and infrequent detection of viremia.

DISCUSSION

In the present study, we described persistent HCV infection in tupaias. Long-term follow-up was performed and revealed histological progression of HCV-related liver disorders in infected tupaias, including steatosis, fibrosis, and cirrhosis, in addition to acute and chronic hepatitis. HCV genomic RNA was detected in animal sera intermittently throughout the entire course of infection. However, HCV RNA was detected in the liver upon sacrifice (3 years postinoculation). Furthermore, HCV RNA in serum contained genomic variants that had diverged from the inoculated virus (see Fig. S1 and S2 in the supplemental material). These data strongly indicate an established persistent infection in the tupaias studied. All animals exhibited HCV viremia soon after inoculation, yet the viremia was intermittent and accompanied by relatively low RTD-PCR titers compared with equivalent human and chimpanzee infections. The discrepancy between humans and tupaias might be due to host-dependent differences in replication efficiency. Over the course of HCV infection in these tupaias, serum ALT profiles indicated repeated liver injury, probably due to host immune responses mediated by agents such as cytotoxic T lymphocytes rather than direct viral cytopathic effects.

In cases of tupaia infection, experimental inoculations rarely led to sustained viremia, which for most human cases lasts for the entire course of infection. Even the course of infection appeared transient and self-resolved. It seems likely that HCV replication is less compatible with the tupaia host environment. This possibility was substantiated by a previous report by Xu et al. (34), where tissue-cultured virions of cloned genotype 1b, referred to as HCVcc in the paper, could not cause chronic infection with sustained viremia in tupaias. Although HCVcc actually infected most of the inoculated tupaias (83%; 10/12), chronic infection was seen for only a fraction of them (20%; 2/10). In this study, we also tried to detect a humoral response to HCV core antigen. We found that tupaia sera were HCV positive for antibodies only at occasional time points, observable as intermittent steep responses (data not shown). Overall, sustained seroconversion was not seen in this study, probably because HCV propagation in vivo was so limited or well controlled by host immunity. Given that models of HCV propagation are severely limited, the most important and interesting finding of this study is the successful detection of HCV RNA in livers of infected tupaias 3 years after inoculation, indicating that HCV persists in tupaias. Although the limited propagation of HCV in tupaias is a drawback of this model at the present time, the isolation of tupaia-adapted HCV may be feasible by performing multiple infection passages. This possibility is supported by both quasispecies development and successful reinfection.

The chimpanzee is the animal species most closely related to humans, and as a model, it has contributed significantly to our understanding of HCV infection and pathogenesis. However, reproducing HCV pathogenesis in humans or chimpanzees can take as long as 10 to 20 years. The chronically infected tupaias in the present study developed complicated liver disorders in a much shorter time. Using tupaias, with their relatively short life span (3 to 5 years in the laboratory), as a model of HCV infection, we can evaluate HCV pathogenesis and correlate senescence and duration of infection.

The recent development of a primary human hepatocyte xenograft-uPA/SCID mouse model opened up opportunities to test putative antivirals against HCV replication in vivo (10, 17). In this innovative model, human hepatocytes, which are transplanted into the lobe of a mouse liver, can support HCV replication effectively. As a result, the level of circulating HCV RNA is comparable to that of a human patient. However, this mouse model is immunodeficient, and thus, it lacks the interplay between host immunity and viral infection. Therefore, it does not provide a suitable platform for characterizing immune responses to HCV infection.

HCV infection in tupaias represents an important model of HCV infection, particularly for the study of key determinants controlling virus propagation in vivo. The pathogenesis of HCV infection can be substantially different among humans, chimpanzees, and tupaias, and the mechanisms governing these differences are of great interest. Comparative studies of HCV infection in these different species will help us to understand the basic mechanisms of persistent infection.

ACKNOWLEDGMENTS

We thank Masahiro Shuda for helpful assistance and Etsuko Endo for creating the figures. We also thank the staffs of the Departments of Microbiology and Cell Biology and Mitsugu Takahashi for breeding the tupaias.

This study was supported by grants from the Ministry of Education, Culture, Sports, Science and Technology of Japan; the Program for Promotion of Fundamental Studies in Health Sciences of the Pharmaceuticals and Medical Devices Agency of Japan; and the Ministry of Health, Labor and Welfare of Japan.

REFERENCES

1. **Abe, K., T. Kurata, Y. Teramoto, J. Shiga, and T. Shikata.** 1993. Lack of susceptibility of various primates and woodchucks to hepatitis C virus. J. Med. Primatol. **22**:433–434.
2. **Aoki, Y., H. Aizaki, T. Shimoike, H. Tani, K. Ishii, I. Saito, Y. Matsuura, and T. Miyamura.** 1998. A human liver cell line exhibits efficient translation of HCV RNAs produced by a recombinant adenovirus expressing T7 RNA polymerase. Virology **250**:140–150.
3. **Chomczynski, P., and N. Sacchi.** 1987. Single-step method of RNA isolation by acid guanidinium thiocyanate-phenol-chloroform extraction. Anal. Biochem. **162**:156–159.
4. **Choo, Q. L., G. Kuo, A. J. Weiner, L. R. Overby, D. W. Bradley, and M. Houghton.** 1989. Isolation of a cDNA clone derived from a blood-borne non-A, non-B viral hepatitis genome. Science **244**:359–362.
5. **Dash, S., G. Kalkeri, H. M. McClure, R. F. Garry, S. Clejan, S. N. Thung, and K. K. Murthy.** 2001. Transmission of HCV to a chimpanzee using virus

particles produced in an RNA-transfected HepG2 cell culture. J. Med. Virol. 65:276–281.
6. **Flugge, P., E. Fuchs, E. Gunther, and L. Walter.** 2002. MHC class I genes of the tree shrew Tupaia belangeri. Immunogenetics 53:984–988.
7. **Goldsmith, E. I.** 1978. The convention on international trade in endangered species of wild fauna and flora. J. Med. Primatol. 7:122–124.
8. **Hong, Z., M. Beaudet-Miller, R. E. Lanford, B. Guerra, J. Wright-Minogue, A. Skelton, B. M. Baroudy, G. R. Reyes, and J. Y. Lau.** 1999. Generation of transmissible hepatitis C virions from a molecular clone in chimpanzees. Virology 256:36–44.
9. **Hoofnagle, J. H.** 2002. Course and outcome of hepatitis C. Hepatology 36:S21–S29.
10. **Inoue, K., T. Umehara, U. T. Ruegg, F. Yasui, T. Watanabe, H. Yasuda, J. M. Dumont, P. Scalfaro, M. Yoshiba, and M. Kohara.** 2007. Evaluation of a cyclophilin inhibitor in hepatitis C virus-infected chimeric mice in vivo. Hepatology 45:921–928.
11. **Ishak, K., A. Baptista, L. Bianchi, F. Callea, J. De Groote, F. Gudat, H. Denk, V. Desmet, G. Korb, R. N. MacSween, et al.** 1995. Histological grading and staging of chronic hepatitis. J. Hepatol. 22:696–699.
12. **Ito, T., K. Yasui, J. Mukaigawa, A. Katsume, M. Kohara, and K. Mitamura.** 2001. Acquisition of susceptibility to hepatitis C virus replication in HepG2 cells by fusion with primary human hepatocytes: establishment of a quantitative assay for hepatitis C virus infectivity in a cell culture system. Hepatology 34:566–572.
13. **Kock, J., M. Nassal, S. MacNelly, T. F. Baumert, H. E. Blum, and F. von Weizsacker.** 2001. Efficient infection of primary tupaia hepatocytes with purified human and woolly monkey hepatitis B virus. J. Virol. 75:5084–5089.
14. **Kolykhalov, A. A., E. V. Agapov, K. J. Blight, K. Mihalik, S. M. Feinstone, and C. M. Rice.** 1997. Transmission of hepatitis C by intrahepatic inoculation with transcribed RNA. Science 277:570–574.
15. **Major, M. E., and S. M. Feinstone.** 1997. The molecular virology of hepatitis C. Hepatology 25:1527–1538.
16. **Marcellin, P., T. Asselah, and N. Boyer.** 2002. Fibrosis and disease progression in hepatitis C. Hepatology 36:S47–S56.
17. **Mercer, D. F., D. E. Schiller, J. F. Elliott, D. N. Douglas, C. Hao, A. Rinfret, W. R. Addison, K. P. Fischer, T. A. Churchill, J. R. Lakey, D. L. Tyrrell, and N. M. Kneteman.** 2001. Hepatitis C virus replication in mice with chimeric human livers. Nat. Med. 7:927–933.
18. **Nascimbeni, M., E. Mizukoshi, M. Bosmann, M. E. Major, K. Mihalik, C. M. Rice, S. M. Feinstone, and B. Rehermann.** 2003. Kinetics of CD4+ and CD8+ memory T-cell responses during hepatitis C virus rechallenge of previously recovered chimpanzees. J. Virol. 77:4781–4793.
19. **Pawlotsky, J. M.** 2002. Use and interpretation of virological tests for hepatitis C. Hepatology 36:S65–S73.
20. **Ren, S., and M. Nassal.** 2001. Hepatitis B virus (HBV) virion and covalently closed circular DNA formation in primary tupaia hepatocytes and human hepatoma cell lines upon HBV genome transduction with replication-defective adenovirus vectors. J. Virol. 75:1104–1116.
21. **Seeff, L. B.** 2002. Natural history of chronic hepatitis C. Hepatology 36:S35–S46.
22. **Shimayama, T., S. Nishikawa, and K. Taira.** 1995. Generality of the NUX rule: kinetic analysis of the results of systematic mutations in the trinucleotide at the cleavage site of hammerhead ribozymes. Biochemistry 34:3649–3654.
23. **Shimizu, Y. K., H. Igarashi, T. Kanematu, K. Fujiwara, D. C. Wong, R. H. Purcell, and H. Yoshikura.** 1997. Sequence analysis of the hepatitis C virus genome recovered from serum, liver, and peripheral blood mononuclear cells of infected chimpanzees. J. Virol. 71:5769–5773.
24. **Shimizu, Y. K., A. Iwamoto, M. Hijikata, R. H. Purcell, and H. Yoshikura.** 1992. Evidence for in vitro replication of hepatitis C virus genome in a human T-cell line. Proc. Natl. Acad. Sci. USA 89:5477–5481.
25. **Suh, Y. A., P. K. Kumar, K. Taira, and S. Nishikawa.** 1993. Self-cleavage activity of the genomic HDV ribozyme in the presence of various divalent metal ions. Nucleic Acids Res. 21:3277–3280.
26. **Takeuchi, T., A. Katsume, T. Tanaka, A. Abe, K. Inoue, K. Tsukiyama-Kohara, R. Kawaguchi, S. Tanaka, and M. Kohara.** 1999. Real-time detection system for quantification of hepatitis C virus genome. Gastroenterology 116:636–642.
27. **Tanaka, T., N. Kato, M. J. Cho, K. Sugiyama, and K. Shimotohno.** 1996. Structure of the 3′ terminus of the hepatitis C virus genome. J. Virol. 70:3307–3312.
28. **Thomson, M., M. Nascimbeni, M. B. Havert, M. Major, S. Gonzales, H. Alter, S. M. Feinstone, K. K. Murthy, B. Rehermann, and T. J. Liang.** 2003. The clearance of hepatitis C virus infection in chimpanzees may not necessarily correlate with the appearance of acquired immunity. J. Virol. 77:862–870.
29. **Tsukiyama-Kohara, K., N. Iizuka, M. Kohara, and A. Nomoto.** 1992. Internal ribosome entry site within hepatitis C virus RNA. J. Virol. 66:1476–1483.
30. **Tsukiyama-Kohara, K., S. Tone, I. Maruyama, K. Inoue, A. Katsume, H. Nuriya, H. Ohmori, J. Ohkawa, K. Taira, Y. Hoshikawa, F. Shibasaki, M. Reth, Y. Minatogawa, and M. Kohara.** 2004. Activation of the CKI-CDK-Rb-E2F pathway in full genome hepatitis C virus-expressing cells. J. Biol. Chem. 279:14531–14541.
31. **Walter, E., R. Keist, B. Niederost, I. Pult, and H. E. Blum.** 1996. Hepatitis B virus infection of tupaia hepatocytes in vitro and in vivo. Hepatology 24:1–5.
32. **Wasley, A., and M. J. Alter.** 2000. Epidemiology of hepatitis C: geographic differences and temporal trends. Semin. Liver Dis. 20:1–16.
33. **Xie, Z. C., J. I. Riezu-Boj, J. J. Lasarte, J. Guillen, J. H. Su, M. P. Civeira, and J. Prieto.** 1998. Transmission of hepatitis C virus infection to tree shrews. Virology 244:513–520.
34. **Xu, X., H. Chen, X. Cao, and K. Ben.** 2007. Efficient infection of tree shrew (Tupaia belangeri) with hepatitis C virus grown in cell culture or from patient plasma. J. Gen. Virol. 88:2504–2512.
35. **Yanagi, M., R. H. Purcell, S. U. Emerson, and J. Bukh.** 1997. Transcripts from a single full-length cDNA clone of hepatitis C virus are infectious when directly transfected into the liver of a chimpanzee. Proc. Natl. Acad. Sci. USA 94:8738–8743.
36. **Yanagi, M., M. St Claire, M. Shapiro, S. U. Emerson, R. H. Purcell, and J. Bukh.** 1998. Transcripts of a chimeric cDNA clone of hepatitis C virus genotype 1b are infectious in vivo. Virology 244:161–172.
37. **Zhao, X., Z. Y. Tang, B. Klumpp, G. Wolff-Vorbeck, H. Barth, S. Levy, F. von Weizsacker, H. E. Blum, and T. F. Baumert.** 2002. Primary hepatocytes of Tupaia belangeri as a potential model for hepatitis C virus infection. J. Clin. Invest. 109:221–232.

GASTROENTEROLOGY 2009;137:285–296

BASIC—LIVER, PANCREAS, AND BILIARY TRACT

Hepatitis C Virus and Disrupted Interferon Signaling Promote Lymphoproliferation via Type II CD95 and Interleukins

KEIGO MACHIDA,[*,‡,§] KYOKO TSUKIYAMA-KOHARA,[*,‖] SATOSHI SEKIGUCH,[*] EIJI SEIKE,[¶] SHIGENOBU TÓNE,[#] YUKIKO HAYASHI,[**] YOSHIMI TOBITA,[*] YURI KASAMA,[‖] MASUMI SHIMIZU,[‡‡] HIDEMI TAKAHASHI,[‡‡] CHYOJI TAYA,[§§] HIROMICHI YONEKAWA,[§§] NOBUYUKI TANAKA,[‡,‖‖] and MICHINORI KOHARA[*]

*Department of Microbiology and Cell Biology, Tokyo Metropolitan Institute of Medical Science, Tokyo, Japan; ‡Department of Immunology, Graduate School of Medicine and Faculty of Medicine, University of Tokyo, Tokyo, Japan; §Department of Molecular Microbiology and Immunology, Keck School of Medicine, University of Southern California, Los Angeles, California; ‖Department of Experimental Phylaxiology, Faculty of Medical and Pharmaceutical Sciences, Kumamoto University, Kumamoto, Japan; ¶Department of Internal Medicine, Self-Defense Forces Central Hospital, Tokyo, Japan; #Department of Biochemistry, Kawasaki Medical School, Okayama, Japan; **Department of Pathology, Tokyo Metropolitan Komagome Hospital, Tokyo, Japan; ‡‡Department of Microbiology and Immunology, Nippon Medical School, Tokyo, Japan; §§Laboratory of Animal Science, Tokyo Metropolitan Institute of Medical Science, Tokyo, Japan; and ‖‖Department of Molecular Oncology, Institute of Gerontology, Nippon Medical School, Kanagawa, Japan*

BACKGROUND & AIMS: The molecular mechanisms of lymphoproliferation associated with the disruption of interferon (IFN) signaling and chronic hepatitis C virus (HCV) infection are poorly understood. Lymphomas are extrahepatic manifestations of HCV infection; we sought to clarify the molecular mechanisms of these processes. **METHODS:** We established interferon regulatory factor-1–null (irf-$1^{-/-}$) mice with inducible and persistent expression of HCV structural proteins (irf-1/CN2 mice). All the mice (n = 900) were observed for at least 600 days after Cre/loxP switching. Histologic analyses, as well as analyses of lymphoproliferation, sensitivity to Fas-induced apoptosis, colony formation, and cytokine production, were performed. Proteins associated with these processes were also assessed. **RESULTS:** *Irf-1*/CN2 mice had extremely high incidences of lymphomas and lymphoproliferative disorders and displayed increased mortality. Disruption of *irf-1* reduced the sensitivity to Fas-induced apoptosis and decreased the levels of caspases-3/7 and caspase-9 messenger RNA species and enzymatic activities. Furthermore, the *irf-1*/CN2 mice showed decreased activation of caspases-3/7 and caspase-9 and increased levels of interleukin (IL)-2, IL-10, and Bcl-2, as well as increased Bcl-2 expression, which promoted oncogenic transformation of lymphocytes. IL-2 and IL-10 were induced by the HCV core protein in splenocytes. **CONCLUSIONS: Disruption of IFN signaling resulted in development of lymphoma, indicating that differential signaling occurs in lymphocytes compared with liver. This mouse model, in which HCV expression and disruption of IFN signaling synergize to promote lymphoproliferation, will be an important tool for the development of therapeutic agents that target the lymphoproliferative pathway.**

More than 175 million people worldwide are infected with hepatitis C virus (HCV), which is a positive-strand RNA virus that infects both hepatocytes and peripheral blood mononuclear cells.[1–4] Chronic hepatitis infection can lead to hepatitis, cirrhosis, hepatocellular carcinoma, and lymphoproliferative diseases, such as B-cell non-Hodgkin's lymphomas and mixed cryoglobulinemia.[5–10] The current therapy for chronic HCV infection involves treatment with type I interferon (IFN) and derivatives of IFN, such as pegylated IFN.[11] Treatment with type I IFN is associated with regression of lymphoma in patients with hepatitis C.[12] However, more than 50% of HCV-infected individuals are resistant to treatment, which indicates that the inhibition of IFN signal transduction facilitates the persistent expression of HCV proteins by hepatocytes.

Transgenic mice that express the HCV core protein have been established using a promoter derived from hepatitis B virus,[13] whereas mice that express structural or complete viral proteins have been established using promoters derived from the albumin gene.[14] These mice are immunotolerant to the transgene and do not develop hepatic inflammation, although they do develop age-related hepatic steatosis and hepatocellular carcinomas. We also developed a transgenic mouse model in which the HCV complementary DNA, including viral genes that encode the core, E1, E2, and NS2 proteins, was conditionally expressed by the Cre/*lox*P system (CN2 mice).[15]

Abbreviations used in this paper: IFN, interferon; IL, interleukin; IRF, interferon-regulatory factor; PCR, polymerase chain reaction; WT, wild-type.

© 2009 by the AGA Institute
0016-5085/09/$36.00
doi:10.1053/j.gastro.2009.03.061

The conditional expression of HCV proteins protected mice from Fas-mediated lethal acute liver failure by inhibiting cytochrome *c* release from the mitochondria.[16] However, the expression of HCV in these mice was usually lost after 21 days. Therefore, an animal model of persistent HCV protein expression is required to examine the effects of chronic HCV infection in vivo.

IFN signaling mediates tumor suppressor effects and antiviral responses and is regulated by key transcription factors of the interferon-regulatory factor (IRF) protein family, including Irf-1, -2, -3, -7, and -9. Targeted disruption of *irf-1* results in aberrant lymphocyte development and a marked reduction in the number of $CD8^+$ T cells in the peripheral blood, spleen, and lymph nodes.[17] In addition, natural killer cell development is impaired in *irf-1*$^{-/-}$ mice.[18] The mechanisms by which HCV infection induces IFN resistance and influences the development of lymphomas are poorly understood. Therefore, in the present study, we established an *irf-1*$^{-/-}$ CN2 mouse model of persistent HCV expression, which allows investigation of the effects of HCV on lymphatic tissue tumor development.

Materials and Methods

Animal Experiments

Wild-type (WT), CN2, *irf-1*$^{-/-}$, and *Mx1-cre* mice were maintained in conventional animal housing under specific pathogen-free conditions. AxCANCre and AxCAw1 were obtained from Dr Izumu Saito (University of Tokyo).[15] To elicit Fas-induced liver damage, adult mice were injected intravenously with 10 μg of purified hamster monoclonal antibody against mouse Fas (clone Jo2; BD Biosciences, San Diego, CA) in 200 μL of phosphate-buffered saline. All animal experiments were performed according to the guidelines of the Tokyo Metropolitan Institute of Medical Science or Kumamoto University Subcommittee for Laboratory Animal Care. The protocol was approved by an institutional review board. Detailed procedures, including induction of the HCV transgene by poly(I:C) in CN2-29 Mx1-Cre mice, are described in Supplementary Materials and Methods.

Measurements of Caspase Activities

The cytosolic splenocyte fractions were isolated as described,[16] and the detailed procedures are described in the Supplementary Material and Methods.

Lentiviral Vectors and Infection

Isolated splenocytes from WT or *irf-1*$^{-/-}$ mice (total of 10^7 cells) were infected with recombinant lentiviruses that express HCV core, E1, E2, NS2, *lacZ*, and empty vector, respectively. One day after infection, cells were selected with puromycin (final concentration of 1 μg/mL). After 5 days of puromycin selection, viable cells were examined.

Baculovirus Expression and Purification of HCV Core, E1, and E2 Proteins

The E1 and E2 sequences from a genotype 1a isolate (strain H77)[19] and a genotype 1b isolate (strain HC-J4),[20] without the C-terminal transmembrane domains but containing the His_6 tag at the C terminus, were cloned into a transfer vector (pBlueBacHis2; Invitrogen, Carlsbad, CA). The expression of recombinant core, E1, and E2 proteins in insect cells and their purification have been described previously.[21]

Results

Viral Protein Expression and Disruption of irf-1 *Synergistically Increase the Development of Lymphoproliferative Disorders*

To clarify the in vivo effects of HCV protein expression, we examined the survival of mice that carry the CN2 transgene (CN2-8, CN2-29).[15] The experimental design is shown in Figure 1*A* (total number of mice, 900). Without Cre/*lox*P switching, the animals that carry the HCV transgene (CN2-8 and CN2-29: core, E1, E2, and NS2 proteins) appeared healthy and developed normally.[15] All of the transgene carriers were observed for at least 600 days after Cre/*lox*P switching (Figure 1*A*). Administration of a recombinant adenovirus that expresses *cre* (AxCANCre) induced the efficient recombination of CN2 transgenes in the hepatocytes from CN2 and *irf-1*$^{-/-}$ CN2 mice (Figure 1*B*). Recombination produced the floxed CN2 transgene (3.3 kilobases) and was completed within 4–7 days; it diminished before day 21 in CN2 mice but persisted in *irf-1*$^{-/-}$ CN2 mice. The expression of core protein in the hepatocytes of CN2 mice peaked on day 7 and decreased to an undetectable level by day 21 (Supplementary Figure 1*A*). The expression of core protein in hepatocytes coincided with a high level of inflammation, as determined by measurements of serum alanine aminotransferase activity (Supplementary Figure 1*A* and data not shown). The HCV core protein was detected in CN2-8 mice 4–14 days after the administration of AxCANCre, and disruption of *irf-1* ensured core protein expression for more than 500 days (Supplementary Figure 1*A* and 1*B*). Therefore, *irf-1* disruption allowed efficient and persistent expression of HCV proteins. HCV core protein gene expression was confirmed by reverse-transcription polymerase chain reaction (PCR) of livers, splenocytes, and peripheral blood monocytes (Supplementary Figure 1C). AxCANCre administration to the transgenic mouse induced the efficient expression of HCV transgenes in lymphocytes and splenocytes (Supplementary Figure 1C).

The survival rate of WT mice injected with the *cre*-adenovirus (AxCANCre) (Figure 1C) or control adenovirus (AxCAw1) (data not shown) was higher than that of the transgenic mice (CN2-8 and CN2-29), which excludes the possibility that the recombinant adenovirus affec-

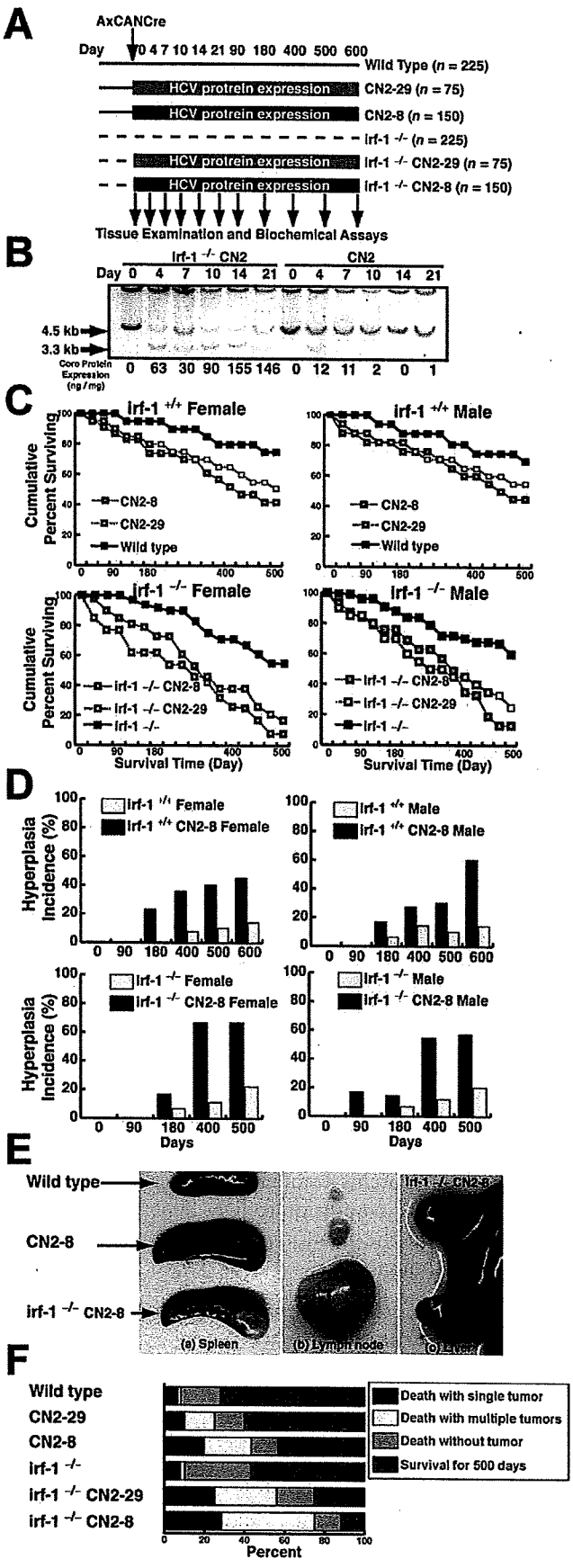

ted the results. More than 75% of the WT mice injected with AxCANCre survived to day 500, whereas the HCV-expressing mice had lower survival rates. The *irf-1*$^{-/-}$ CN2-8 and *irf-1*$^{-/-}$ CN2-29 strains had even lower survival rates, indicating that persistent HCV protein expression in combination with *irf-1* disruption significantly decreases survival (Figure 1C).

Lymphoproliferative Disorders Are Accelerated With Age and Level of Viral Protein Expression

To determine the mechanism underlying the increased mortality caused by persistent HCV protein expression in *irf-1*$^{-/-}$ CN2 mice, we examined the kinetics of dysplasia (Figure 1*D*). Strikingly, 67% of the female *irf-1*$^{-/-}$ CN2 mice and 70% of the male *irf-1*$^{-/-}$ CN2 mice developed tumors 400 days after the administration of AxCANCre. Some of the *irf-1*$^{-/-}$ CN2 mice developed hyperplasia of the lymph nodes, and these tumors developed much earlier than the tumors in their *irf-1*$^{+/+}$ or CN2 counterparts (Figure 1*D*). Aberrant cell proliferation developed randomly among the male and female carrier animals between day 180 and day 600. On day 400 after Cre/*lox*P switching, the average weights of the spleens of the WT, CN2, and *irf-1*$^{-/-}$ CN2 mice were 90, 160, and 310 mg, respectively. The disruption of *irf-1* aggravated the HCV-induced spontaneous proliferative disturbances in lymphatic tissues. The number of CN2 mice that died with at least one tumor and the number of tumors per

Figure 1. Disruption of *irf-1* enhances oncogenic potential in combination with HCV transgene expression. (*A*) Experimental design for the animal model. Transgenic mice and their nontransgenic littermates (10–14 weeks of age) were administered the *Cre*-expressing adenovirus (AxCANCre) and killed after 4, 7, 10, 14, 21, 90, 120, 400, 500, or 600 days. (*B*) Southern blot analysis of hepatocyte DNA from mice derived by crossing *irf-1*$^{-/-}$ and HCV-transgenic (CN2) mice. Genomic DNA samples from WT (+/+) and CN2 mouse hepatocytes were digested with *Xba*I and subjected to Southern blot analysis using a radiolabeled genomic flanking probe to determine the rate of recombination of the HCV transgene construct (3.3-kilobase fragment). Disruption of *irf-1* allows persistent expression of HCV proteins. The effects of HCV protein expression on the survival rates of male and female *irf-1*$^{-/-}$ and *irf-1*$^{+/+}$ CN2 mice are shown. (*C*) Kaplan–Meier survival curves for WT mice, *irf-1*$^{-/-}$ mice, CN2 transgenic mouse strains 8 and 29, and *irf-1*$^{-/-}$ CN2-8 and CN-29 mice following infection with a recombinant adenovirus that expresses *cre* (AxCANCre). (*D*) HCV protein expression enhances hyperplasia in male and female CN2 and *irf-1*$^{-/-}$ CN2 mice. The occurrence of hyperplasia was monitored every 7 days for 600 days following the administration of AxCANCre. (*E*) Spleens (*a*) and lymph nodes (*b*) from age-matched WT, CN2, and *irf-1*$^{-/-}$ CN2 mice 500 days after the administration of AxCANCre. (*c*) Liver from the same *irf-1*$^{-/-}$ CN2 mouse (developing severe lymphadenopathy and splenomegaly) following the administration of AxCANCre. (*F*) The cause of death in CN2 transgenic mice with hyperplasias. Mice of each genotype (n = 150) were monitored up to day 600 after the administration of AxCANCre, and necropsies were performed to determine the number of tumors. Tumors included thymomas, splenomas, lymphomas, and hepatocellular carcinomas.